NAVAL POSTGRADUATE SCHOOL

MONTEREY, CALIFORNIA

THESIS

FLUID STRUCTURE INTERACTION EFFECT ON SANDWICH COMPOSITES

by

Michael A. Violette

September 2011

Thesis Advisor: Young W. Kwon
Second Reader: Jarema M. Didoszak

Approved for public release; distribution is unlimited

THIS PAGE INTENTIONALLY LEFT BLANK

REPORT DOCUMENTATION PAGE			Form Approved OMB No. 0704–0188
Public reporting burden for this collection of information is estimated to average 1 hour per response, including the time for reviewing instruction, searching existing data sources, gathering and maintaining the data needed, and completing and reviewing the collection of information. Send comments regarding this burden estimate or any other aspect of this collection of information, including suggestions for reducing this burden, to Washington headquarters Services, Directorate for Information Operations and Reports, 1215 Jefferson Davis Highway, Suite 1204, Arlington, VA 22202–4302, and to the Office of Management and Budget, Paperwork Reduction Project (0704–0188) Washington DC 20503.			
1. AGENCY USE ONLY *(Leave blank)*	**2. REPORT DATE** September 2011	**3. REPORT TYPE AND DATES COVERED** Master's Thesis	
4. TITLE AND SUBTITLE Fluid Structure Interaction Effect on Sandwich Composites		**5. FUNDING NUMBERS**	
6. AUTHOR(S) Michael A. Violette			
7. PERFORMING ORGANIZATION NAME(S) AND ADDRESS(ES) Naval Postgraduate School Monterey, CA 93943–5000		**8. PERFORMING ORGANIZATION REPORT NUMBER**	
9. SPONSORING /MONITORING AGENCY NAME(S) AND ADDRESS(ES) N/A		**10. SPONSORING/MONITORING AGENCY REPORT NUMBER**	
11. SUPPLEMENTARY NOTES The views expressed in this thesis are those of the author and do not reflect the official policy or position of the Department of Defense or the U.S. Government. IRB Protocol number _____N/A_____.			
12a. DISTRIBUTION / AVAILABILITY STATEMENT Approved for public release; distribution is unlimited		**12b. DISTRIBUTION CODE**	

13. ABSTRACT (maximum 200 words)

The objective of this research is to examine the fluid structure interaction (FSI) effect on composite sandwich structures under a low velocity impact. The primary sandwich composite used in this study was a 6.35-mm balsa core and a multi-ply symmetrical plain weave 6 oz E-glass skin. The specific geometry of the composite was a 305 by 305 mm square with clamped boundary conditions. Using a uniquely designed vertical drop-weight testing machine, there were three fluid conditions in which these experiments focused. The first of these conditions was completely dry (or air) surrounded testing. The second condition was completely water submerged. The final condition was a wet top/air-backed surrounded test. The tests were conducted progressively from a low to high drop height to best conclude the onset and spread of damage to the sandwich composite when impacted with the test machine. The measured output of these tests was force levels and multi-axis strain performance. The collection and analysis of this data will help to increase the understanding of the study of sandwich composites, particularly in a marine environment.

14. SUBJECT TERMS Fluid Structure Interaction, FSI, composite, balsa, low velocity impact, sandwich composites, VARTM, Vacuum Assisted Resin Transfer Molding			**15. NUMBER OF PAGES** 73
			16. PRICE CODE
17. SECURITY CLASSIFICATION OF REPORT Unclassified	**18. SECURITY CLASSIFICATION OF THIS PAGE** Unclassified	**19. SECURITY CLASSIFICATION OF ABSTRACT** Unclassified	**20. LIMITATION OF ABSTRACT** UU

NSN 7540–01–280–5500 Standard Form 298 (Rev. 2–89)
Prescribed by ANSI Std. 239–18

THIS PAGE INTENTIONALLY LEFT BLANK

Approved for public release; distribution is unlimited

FLUID STRUCTURE INTERACTION EFFECT ON SANDWICH COMPOSITE STRUCTURES

Michael A. Violette
Lieutenant Commander, United States Navy
B.S., Virginia Military Institute, 1998

Submitted in partial fulfillment of the
requirements for the degree of

MASTER OF SCIENCE IN MECHANICAL ENGINEERING

from the

NAVAL POSTGRADUATE SCHOOL
September 2011

Author: Michael A. Violette

Approved by: Young W. Kwon
Thesis Advisor

Jarema M. Didoszak
Second Reader

Knox T. Millsaps
Chair, Department of Mechanical and Aerospace Engineering

THIS PAGE INTENTIONALLY LEFT BLANK

ABSTRACT

The objective of this research is to examine the fluid structure interaction (FSI) effect on composite sandwich structures under a low velocity impact. The primary sandwich composite used in this study was a 6.35-mm balsa core and a multi-ply symmetrical plain weave 6 oz E-glass skin. The specific geometry of the composite was a 305 by 305 mm square with clamped boundary conditions. Using a uniquely designed vertical drop-weight testing machine, there were three fluid conditions in which these experiments focused. The first of these conditions was completely dry (or air) surrounded testing. The second condition was completely water submerged. The final condition was a wet top/air-backed surrounded test. The tests were conducted progressively from a low to high drop height to best conclude the onset and spread of damage to the sandwich composite when impacted with the test machine. The measured output of these tests was force levels and multiaxis strain performance. The collection and analysis of this data will help to increase the understanding of the study of sandwich composites, particularly in a marine environment.

THIS PAGE INTENTIONALLY LEFT BLANK

TABLE OF CONTENTS

LIST OF FIGURES

LIST OF TABLES

THIS PAGE INTENTIONALLY LEFT BLANK

ACKNOWLEDGMENTS

I would like to thank Dr. Kwon for his mentorship, guidance, and his patience throughout the course of this thesis. His ability to quickly guide me through and bring clarity to seemingly endless pages of measured data is amazing. Additionally, this thesis would not have been possible without the incredible technical support provided to me by Tom Christian. Even in "retirement," he selflessly shared his years of experience with me.

My parents have been and remain a bedrock of support and guidance to me. I could have no greater personal and professional mentors than my mother and father.

Most importantly, I would like to thank my beautiful wife, Courtney, and my three wonderful children, Charlie, Maryellen, and Teddy. Without Courtney, none of my professional accomplishments would be achievable. Charlie, Maryellen, and Teddy are truly an inspiration that each generation should continue to seek knowledge in the hope that we leave behind a better world.

THIS PAGE INTENTIONALLY LEFT BLANK

I. INTRODUCTION

A. BACKGROUND

The use of composite materials in fabrication can be attributed as far back as ancient Egyptian times in the use of straw and bricks, or more recently in the last century with the use of steel rebar in concrete. The goal in either of these applications is the enhanced structural properties of a structure. In the post-Industrial Revolution era, the modern era of composite use began around World War II. Since that time, the research and use of composite materials grew rather modestly until a rapid rise in the 1990s and early 2000s [1].

The aerospace industry, in particular, has been very aggressive in its use of composites in its most critical applications when compared to other industries. NASA's Jet Propulsion Laboratory at the California Institute of Technology lists structural laminate composites as one of its preferred practices for the recently retired Space Shuttle program. Among the chief reasons for the use of composites is the high strength to weight ratio [2].

The military marine industry is seeking to follow the aerospace example and has been using composites in naval architecture since the post–World War II era. Primarily, the use of composites was limited to component structures or smaller patrol craft. The last decade has significantly changed the paradigm to how the marine industry is building military ships and has seen an all composite construction in European military ships up to 90 meters in length [1]. The U.S. Navy presently is making significant strides in the use of composites in critical combat hardware. The first major example aboard a U.S. Navy combatant is the Advanced Enclosed Mast used aboard the *USS Arthur W. Radford* (DD-968) [3]. The *Radford* mast was fully enclosed and constructed entirely of composites and led to the design currently used by the LPD-17 *San Antonio* class amphibious docking ships [4]. Looking ahead and building on the successes of *Radford* and the *San Antonio* class, the Navy has begun construction on the next-generation destroyer: the DDG-1000 *Zumwalt* class. The *Zumwalt* class will include

a seven-story superstructure composed almost entirely of composite materials. The superstructure employed the widely used resin transfer system scheme primarily with carbon fiber/vinyl ester skins and balsa wood and/or foam cores, thus creating a "sandwich" composite.

What is the advantage of using products like wood in a ship's construction? The idea of using balsa wood is more advanced than the construction of the Navy's only other active wooden ship, the now ceremonial, *USS Constitution*. The balsa wood core takes advantage of favorable strength to weight ratios gaining its strength with the reinforcing carbon fiber skins. In addition to the strength to weight advantages, the sandwich composite provides an ability to simplify tooling in construction, reduce corrosion, and reduces the ship's radar cross section [4]. The reduced radar cross section makes the ship significantly stealthier, while the other composite attributes allow for increased range, and an ability to increase payload. The maintenance costs are also likely to be reduced over a lifetime in reduced manufacturing costs and required preventive and corrective maintenance requirements, which in turn reduce the number of crewmembers needed to maintain the ship. Advances are also being made in rudder construction using the same composite technology that may help reduce cavitation resulting in reduced stresses on the ship's rudders [5].

With the rapid increase in the use of composites, the ability to predict potential failure modes and thresholds is critical in designing ships that can meet or exceed expected service life requirements. The major drawback to sandwich composites is a relative lack of ductility when compared to other metallic materials. The damage to composites in a sandwich laminate structure is also frequently undetectable [6]. With this undetected damage, there may be no observable reduction in the mechanical properties until catastrophic failure occurs. The materials used in this study were selected to best detect the onset of damage, and reduced mechanical properties while modeling the current technologies being used in U.S. naval applications. Material selection and methodologies will be discussed in subsequent chapters.

B. OBJECTIVES

Given the direction the U.S. Navy with an increased use of sandwich composites, it is the goal of this study to further that endeavor. Recently, experiments conducted by Kwon and Owens [7, 17] and Kwon and McCrillis [8] have studied the fluid structure interaction (FSI) on composites with a carbon fiber plate and balsa core beams respectively. This present study will combine the efforts of the two and examine the FSI on balsa core plate-geometries.

This study will evaluate the dynamic response of a sandwich composite under a low velocity impact. There were three basic conditions used to study these sandwich composites: dry, submerged-water backed, and to a lesser, extent submerged-air backed. It has been shown in previous studies that there is an added mass effect due to the relative difference in densities of a composite in water. The balsa core sandwich composites used in this study are significantly less dense than water. Due to this density differential, it is believed that the added mass effect will be larger on a less dense sandwich composite. There are several indicators that will help to draw a conclusion to the FSI effects on the selected sandwich composites. Most directly, this study will measure the dynamic response through the use of force impact levels and a multi-axis strain response. Additionally, conclusions will be drawn from damage initiation, type, and proliferation through the sample. Taken from the multiaxis strain response, deformation magnitudes, mode shapes, and calculated natural frequencies will help to make conclusions as to the dynamic response of the sandwich composite. In the collection of all of these factors, the study will show that the FSI in water plays a critical role in the composite's performance and thus any composite intended for marine use must be evaluated in this same environment.

THIS PAGE INTENTIONALLY LEFT BLANK

II. EXPERIMENTAL TECHNIQUE

A. SANDWICH COMPOSITE SELECTION

Thirteen sandwich composite samples were constructed and tested for analysis throughout the course of this research. The Naval Surface Warfare Center Carderock Advanced Hull Materials & Structures Technology Division selected the materials for this study for their direct applicability to current shipboard U.S. Navy composite structures. Following the work of Kwon and Owens [7, 17] and Kwon and McCrillis [8], a combination of their research was studied. The chief components of the sandwich composite are the core, skin layers, and resin.

1. Core: Balsa Wood

A 6.35-mm end grain balsa core was used. McCrillis noted that the appearance of balsa wood is similar to that of a butcher block (Figure 1).

Figure 1. "Butcher block" appearance of balsa wood.

McCrillis observed in his study that due to the inhomogeneous qualities of the balsa material that the absorption of resin was unequal and further magnified the inhomogeneous properties of the sandwich composite during testing [8]. ProBalsa Plus is pretreated to reduce the resin absorption during composite manufacturing to minimize large variations in mechanical properties across the sample. As a result, ProBalsa Plus was used as the composite core in this study as well. ProBalsa Plus is characterized as a micro-honeycomb structure with excellent shear and compressive properties. The DIAB Group manufactured the ProBalsa used in this study and provides the properties in Table 1 [9].

Mechanical Properties					
Property	Method	Unit	LD7 Light Weight	PB Standard	HW Heavy Weight
Density	ASTM C 271	kg/m³	90	155	220
		lb/ft³	5.6	9.7	13.8
Compressive Strength [1]	ASTM C 365	MPa	5.4	12.7	21.9
		psi	783	1,842	3,176
Compressive Modulus [1]	ASTM C 365	MPa	1,850	4,100	6,840
		ksi	268	594	992
Tensile Strength [1]	ASTM C 297	MPa	7.0	13.5	20.6
		psi	1,015	1,958	2,987
Shear Strength [1]	ASTM C 273	MPa	1.6	3.0	4.5
		psi	232	435	653
Shear Modulus [1]	ASTM C 273	MPa	96	168	237
		ksi	14	24	34
Thermal Conductivity [2]	ASTM C 377	W/m·K	0.052	0.064	0.086
		Btu·in/(ft²·h·°F)	0.35	0.44	0.60
R-value	Based on +10° K factor	12 mm / 0.5 in	1.4	1.1	0.8
		25 mm / 1.0 in	2.9	2.3	1.7
		51 mm / 2.0 in	5.7	4.5	3.3
1) All values measured at +22°C (+72°F).					
2) Thermal conductivity at +10°C (+50°F).					

Table 1. Technical Data for ProBalsa (From [9]).

2. Skin: E-glass

The skin material used in this study was a non-biased, plain weave, 6 oz E-glass. The thickness of the E-glass is 0.236 mm [10]. A variety of weights and weave constructs could be used in the construction of sandwich composites; however, this particular material was selected for its uniform pattern and translucent qualities after it is wetted out during composite manufacturing. A significantly coarser weave pattern was also explored during this study, but the data scatter was significant enough to determine

the tighter weave would produce results that are more consistent. The published material properties of E-glass can vary significantly, however, based on measurement of multiple 10 cm square samples, the density of the e-glass was found to be nominally 842 kg/m^3 for the samples studied.

3. Resin: Vinyl Ester Resin

The particular resin used in this study is Derakane 510A vinyl ester resin. The vinyl ester resin has excellent fire retardant and corrosion resistant qualities making it a natural selection for shipboard applications. The same translucent qualities found in the E-glass are additional benefits of vinyl ester resins. Dererakane 510A has a density of 1230 kg/m^3 and is further characterized by the properties of Table 2 for a clear casting only [11].

Property	SI	US Standard
Tensile Strength	86 MPa	12,300 psi
Tensile Modulus	3.40 GPa	4.93 x 10^5 psi
Tensile Elongation, Yield	4-5%	4-5%
Flexural Strength	150 MPa	21,700 psi
Flexural Modulus	3.60 GPa	5.22 x 10^5 psi
Heat Distortion Temperature[10]	113°C	220°F
Barcol Hardness	40	40

Table 2. Typical Properties of postcured resin clear casting. (From [11]).

In addition to the resin, there are chemical hardening components that contribute to the overall composite manufacturing process [12]. Table 3 identifies specific mixtures based on the ambient conditions. A 40–60 minute gel time was typically used to determine the appropriate hardening mixture.

Temperature		10-20 minutes	20-40 minutes	40-60 minutes
15°-20°C Cool 60s°F	MEKP	2.50%	2.00%	1.25%
	Cobalt	0.30%	0.30%	0.30%
	DMA	0.25%	0.10%	0.05%
21°-26°C Mild 70s °F	MEKP	2.00%	1.25%	1.00%
	Cobalt	0.30%	0.30%	0.20%
	DMA	0.05%		
27°-32°C Warm 80s °F	MEKP	1.50%	1.25%	1.25%
	Cobalt	0.20%	0.20%	0.20%
	DMA	0.05%		
	2,4-P			0.05%

Table 3. Gel times using methyl ethyl ketone peroxide (MEKP) (From [12]).

B. COMPOSITE GEOMETRY

Using the above core materials in the laminate construction, a sample of 305 mm square defined the test area. The actual sample size was determined to best simulate clamped boundary conditions on all four side of the test sample. In order to minimize any movement at the boundary conditions as large as sample as possible given the test apparatus was constructed. For the test apparatus used, the maximum sample size was a rectangular sample: 381 x 457.2 mm. The 305 mm square was centered within this rectangular sample and the area to the outside of the test area was clamped as part of the boundary conditions. The grid scheme in Figure 2 will be utilized throughout the course of this research to specifically identify exact points on the test area. The origin of the test area is placed at the lower left hand corner of the test sample. The orientation of the grid scheme is from the underside of the sample looking up at the dropweight on the test apparatus. The unit spacing is equivalent to one mm.

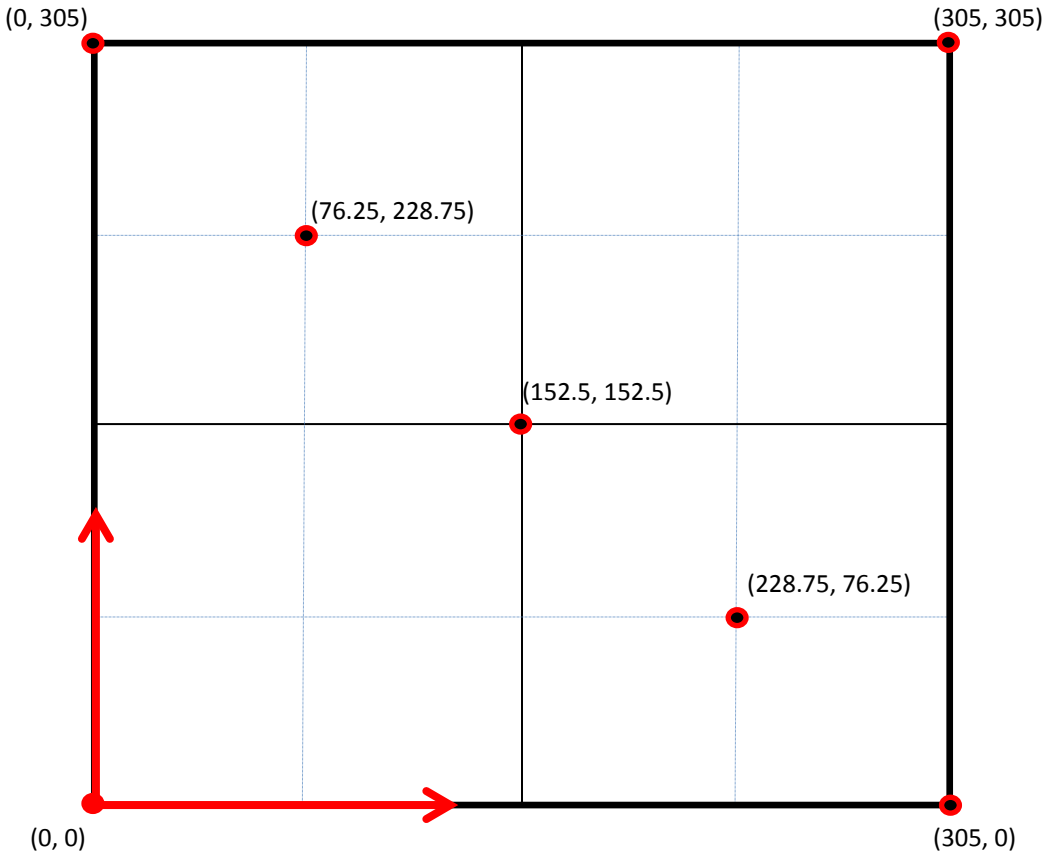

Figure 2. Composite test area grid (bottom view looking up).

The grid reference system in Figure 2 is of particular importance in referencing and comparing specific strain responses for different samples. The impact point for all tests was at the center of the test area (152.5, 152.5).

C. MATERIAL REQUIREMENTS

In addition to the core composite materials, the fabrication of the composite requires additional support material and equipment. Table 4 and Figure 3 outline the materials and equipment required to produce the described square geometry test area plus the additional area required to simulate clamped boundary conditions for the test apparatus.

Composites can be constructed of a variety of materials and thicknesses and various techniques. The quantities listed for materials are specific to the samples created in this study and a unique resin transfer apparatus. Chemical quantities listed are specific

for a manufacturing at an ambient room temperature of around 20° C (68° F). Specific room temperatures varied slightly during each sample production. Nominal laboratory temperatures ranged from 17–20° C throughout the course of this study. Table 3 should be referenced for a desired gel time and chemical solution based on the ambient conditions present at the time of production.

Component	Size	Qty
Pro Balsa Plus (core)	381 mm x 457.2 mm (15 in x 18 in)	1
6 oz E-glass (skin)	381 mm x 457.2 mm (15 in x 18 in)	10
Peel Ply	482.6 mm x (19 in x 22 in)	3
Airtech ® Resinflow 75 Distribution Medium	381 mm x 533.4 (15 in x 21 in)	2
Stretchlon 200 1.5 Vacuum Bag Film	584.2 mm x 660.4 (23 in x 26 in)	1
Derakane 510-A (resin)	n/a	1,000 mL
Methyl Ethyl Ketone Peroxide (MEKP)	n/a	12.5 mL
Cobalt Napthenate (CoNAP)	n/a	3 mL
N, N-Dimethylaniline (DMA)	n/a	0.5 mL
AT-200Y sealant tape	254 cm (100 in)	1
Teflon	482.6 mm x (19 in x 22 in)	1

Table 4. Required materials for VARTM composite production.

VARTM Apparatus Components:
Vacuum pump
Vacuum hose
Spiral wrap
2 Liter resin bucket
Resin trap
Vacuum gage
Glass foundation

Figure 3. Additional required equipment for VARTM composite production.

Other useful equipment that comes in handy during composite production is clamps of various sizes, small free weights (approx. 5 lbs), and duct tape. Each of these materials will help the manufacturer keep the integrity of the vacuum during the resin transfer process.

D. COMPOSITE FABRICATION

1. Vacuum Assisted Resin Transfer Molding (VARTM)

The composites were fabricated using the VARTM process shown in Figure 4. In general, a vacuum bag lamination molding process such as VARTM covers the layers of the composite core (balsa) material and laminate skins (E-glass) with a sealed bagging membrane (sealant tape and Stretchlon 200). The vacuum pump and support equipment evacuate the interior of the membrane, reducing the internal pressure, and allowing standard atmospheric conditions to compress the laminate skins to the core to create a mold [13]. The distribution medium and spiral wrap are used together to assist in the even flow and infusion of the resin across the sample. The Teflon and peel ply allows for easier removal from the glass preparation surface and separation from the molded composite respectively. As the manufacturer becomes more experienced sample preparation time will likely decrease, however, Table 5 shows a nominal range of sample preparation times and required curing times experienced during this study.

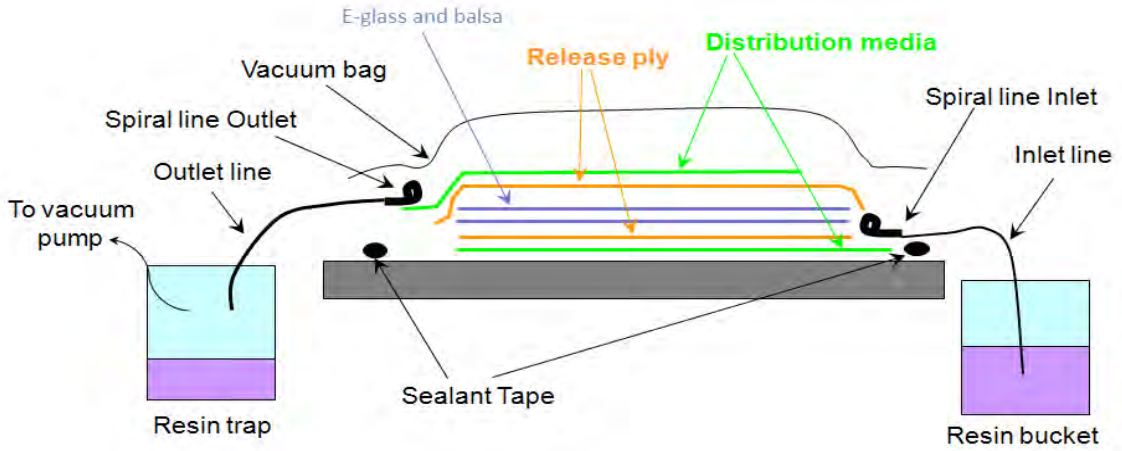

Figure 4. VARTM Lay-up (From [8]).

Procedure	Time
Lay-up (cutting and air evacuation)	1–1.5 hrs
Chemical mixture	10–15 min
Resin Transfer	15–20 min
Post Cure (vacuum on – room temp)	8 hrs
Post Cure (vacuum off - room temp)	24 hrs
Post Cure (elevated temperature)	6 hrs
TOTAL	***Approx. 40 hrs***

Table 5. Nominal prep time for composite sample preparation.

2. Procedure

The VARTM procedure used for the balsa/e-glass sandwich composite is outlined with recommended techniques and hints in the steps below (tabulated in Table 6 for quick reference for future fabrication).

Step 1: Composite Preparation

Cut balsa core to desired size

Cut 10 sheets of E-glass fabric (same size of core)

Cut 3 sheets of peel ply: 4 inches larger in each direction as core material to completely envelope sample and allow an adequate amount material to grab and more easily remove the peel ply and distribution medium after molding and curing process.

Cut 2 sheets of distribution medium: distribution medium was made slightly smaller than peel ply to allow peel ply to prevent jagged edges of distribution medium from piercing vacuum bag during evacuation.

Step 2: Surface Preparation

Lay peel ply (largest surface area) on glass surface and tape edges of glass plate with a continuous line of sealant tape; do not remove backing. Space between sealant tape and edge of peel ply is discretionary. Remove peel ply sheet from glass surface.

Lay out Teflon sheets within boundary of sealant tape to facilitate mold release. Previous theses have recommended waxing glass surface or using Teflon sheets [6,7], but significantly better results were achieved with the Teflon sheets during this study.

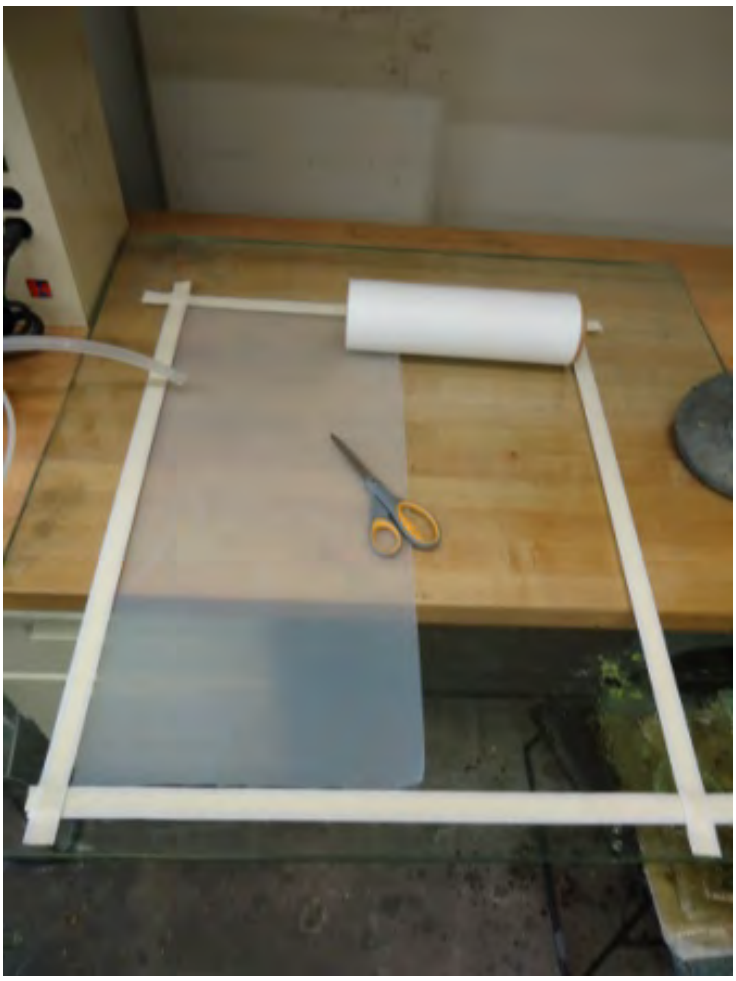

Figure 5. Composite fabrication: Lay out of Teflon sheets after sealant applied to glass surface.

Step 3: Material Layup

Layup material in the following order from bottom to top prior to wetting:

1. distribution medium
2. peel ply
3. 5 sheets E-glass
4. balsa core
5. 5 sheets E-glass
6. peel ply
7. distribution medium
8. peel ply

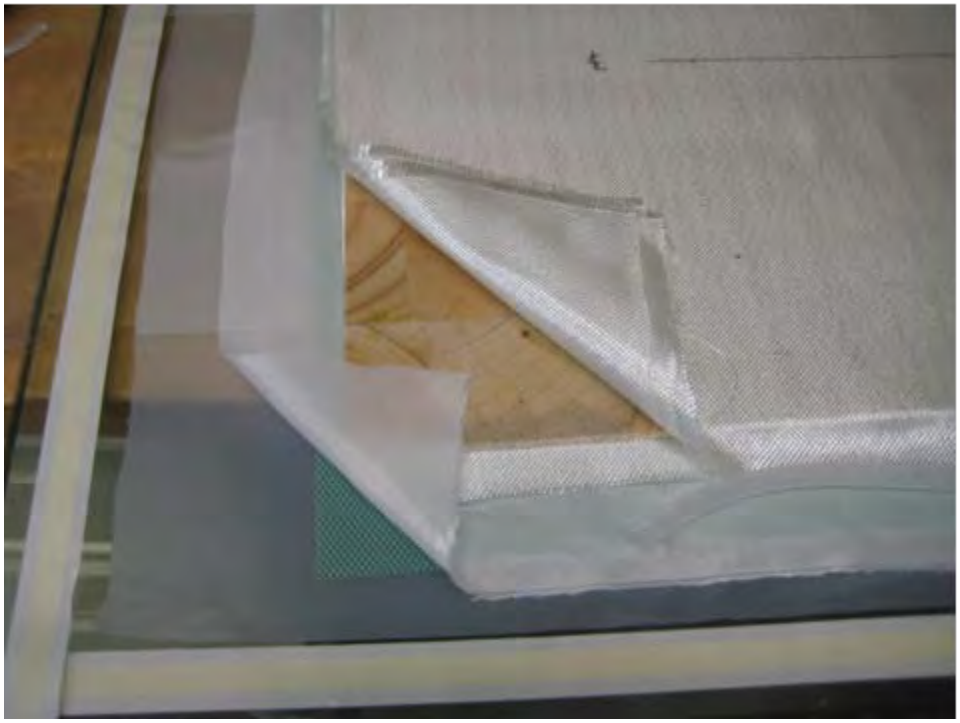

Figure 6. Composite Fabrication: Layup prior to wetting after e-glass skins applied. Yet to be applied from Step 3: peel ply (x2) and distribution medium (After [8]).

Step 4: Vacuum Hose Routing

Cut two pieces of vacuum hose (feed and suction) to lengths necessary to route from resin bucket across sealant tape (feed) and from resin trap across sealant tape at opposite end of sample (suction). Peel back a small portion of the sealant tape to affix the hose to the sealant tape at each end. Pre-wrapping the vacuum hoses with sealant tape where they will cross the sealant tape barrier will significantly improve the ability to

bond the hose with the sealant barrier. The use of free weights, clamps, and duct tape come in handy for keeping the vacuum hoses and sealant tape adhered to the glass surface. Additionally, pre-kinking the feed hose will make it easier to secure the resin transfer process later. Making small kinks in each of the two hoses may also make the vacuum hose routing process easier. The hose is typically shipped and stored in a spiral and wants to return to its stored position; the kinks will "straighten" the hose to the desired routing.

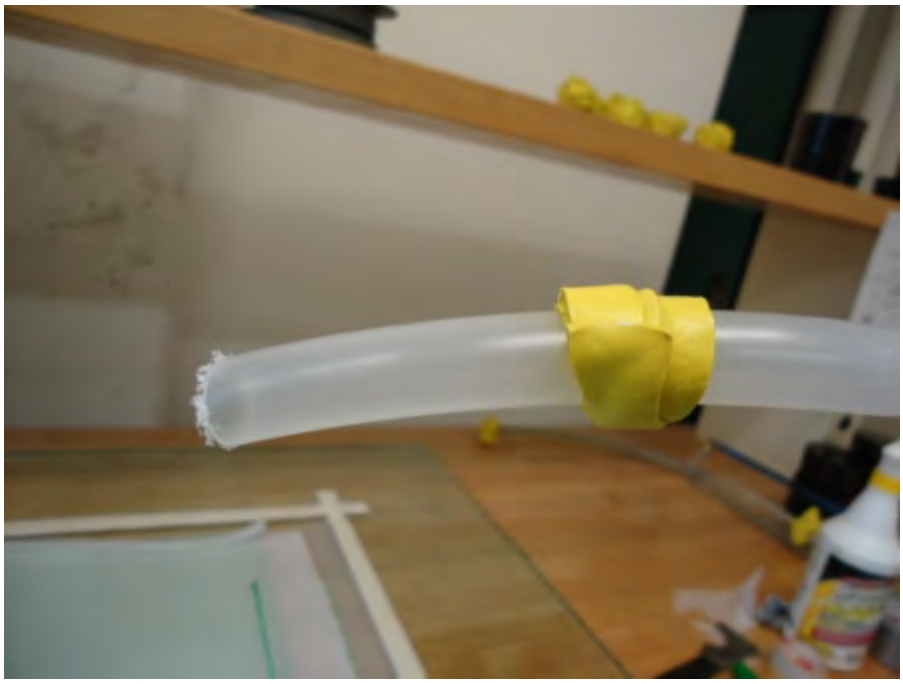

Figure 7. Composite Fabrication: Prewrapping vacuum hoses with sealant tape allows for better adhering to sealant tape on glass surface.

Cut two pieces of spiral wrap the approximate width of the sample plus the distance to insert spiral wrap in the feed and suction hoses approximately 5 cm.

Ensure the spiral wrap is in contact with the distribution medium at each end of the sample. Small pieces of sealant tape may help in keeping the spiral wrap in the desired position. Best results were achieved for the infusion process when the spiral

wrap was on top of the bottom layer of distribution medium at the feed end of the sample and on top of the top layer of distribution medium at the suction end as shown in Figure 4.

Placing sealant tape on any sharp edges of the cut vacuum hoses may also eliminate a possible puncture of the vacuum bag during the resin transfer and post curing process.

Step 5: Create Vacuum

Remove sealant tape backing

Apply vacuum bag across layup. "Tucking" the vacuum bag at the area of the vacuum hose-layup interface first helps to reduce leaks once the bag is applied.

Figure 8. Composite Fabrication: Tucking the vacuum bag around suction hose interface.

Plug feed hose with excess sealant tape. The plugged hose reduces the chance for air to enter the mold at the beginning of the resin transfer process.

Turn on vacuum pump and check and eliminate any leaks. The use of sealant tape and kneading the vacuum bag into the seal are the most effective techniques. The most common sources of leaks are the interfaces of the vacuum hoses at the layup barrier and the interface of the suction hose with the resin trap. A vacuum should remain on the mold from this point forward.

Step 6: Combine Resin Chemicals

Pour 1 L of Derakane 510-A

Add 3 mL of Cobalt (stir)

Add 0.5 mL of DMA (stir)

Add 12.5 mL of MEKP (stir)

Mix the chemical solution thoroughly until the resin reaction is complete and has no more air bubbles.

Step 7: Resin Transfer

Place feed hose in resin solution

Break seal (remove sealant tape) from feed hose

Resin will rapidly be drawn through the hose and be drawn into the spiral wrap and subsequently infuse through the mold.

Continue to monitor and eliminate any leaks through the infusion process.

It may be necessary to angle the feed bucket to keep the hose submerged toward the end of the infusion process as the resin level goes down. Once the sample has been fully infused use the "pre-positioned" kinks in the feed hose to quickly fully kink and clamp the feed hose. Place excess sealant tape on the end of the hose to prevent air from contaminating your sample.

Step 8: Curing

After 8 hours secure the vacuum pump

Allow sample to cure at room temperature for 24 hours

Post cure the sample at 160° F for 6 hours

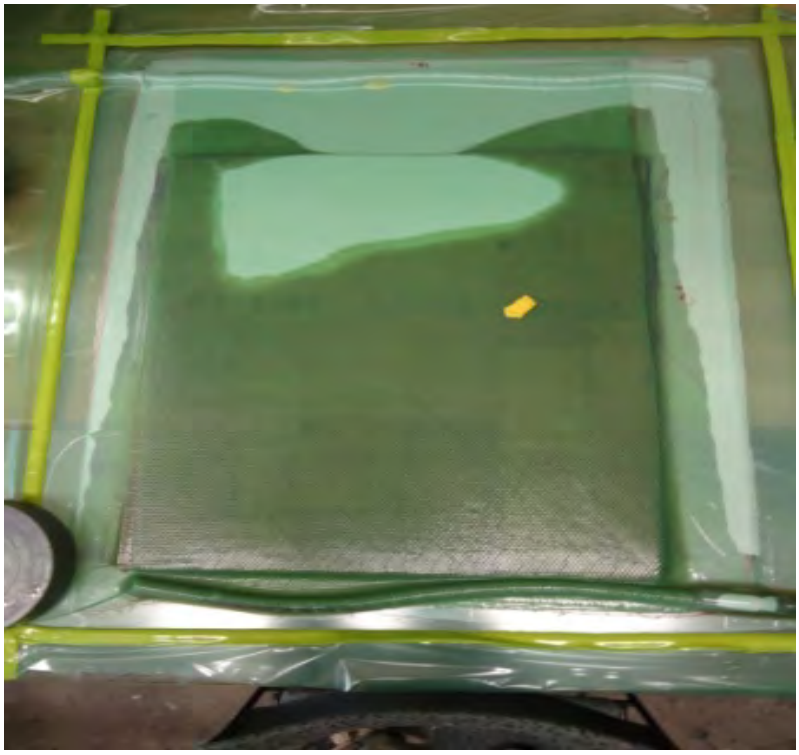

Figure 9. Composite Fabrication: Infusion of resin across sample.

Step 9: Make Ready for Testing

Using the peel ply, remove the distribution medium to expose the skin laminate and core. It was found that allowing the curing process with the peel ply and distribution medium still attached prevented the "pulling" off of any tacky resin from the sample and helped to maintain a uniform application. Because of run-off on the edges of the sample from the resin, it may be required to trim the sample to fit in the test rig. If any are of the core is exposed, it should be treated with a carnuba wax to prevent water intrusion into the sample. The sandwich composite is now ready for testing.

Step 1	***Composite Preparation***
	Cut core material
	Cut skin layers
	Cut peel ply
	Cut distribution medium
Step 2	***Surface Preparation***
	Lay out sealant tape barrier
	Place Teflon within barrier
Step 3	***Material Layup***
	Place distribution medium on top of Teflon
	Place peel play on top of distribution medium
	Place skin laminate skin layers on top of distribution medium
	Place composite core on skin layers
	Place second set of laminate skin layers on top of core
	Place peel ply on laminate skin layers
	Place distribution medium on peel ply
Step 4	***Vacuum Hose Routing***
	Cut spiral wrap and vacuum hose to desired size
	Route hoses and spiral wrap
Step 5	***Create Vacuum***
	Remove sealant tape
	Apply vacuum bag
	Turn on vacuum pump to reach and maintain approximately 30 in Hg
Step 6	***Combine Resin chemicals***
	Mix chemicals stirring continuously; wait for “gas-off” of bubbles
Step 7	***Resin Transfer***
	Place feed hose in resin bucket and remove seal from hose
	Continue transfer until infused over entire sample
	Clamp feed hose
Step 8	***Curing***
	After 8 hours secure vacuum pump
	Cure at room temperature for 24 hours
	Cure at 160° F for six hours
Step 9	***Make ready for testing***
	Remove peel ply and distribution medium
	Trim as necessary
	Apply wax as necessary to exposed core on edges

Table 6. Sandwich composite fabrication summary.

E. STRAIN GAGES

For the majority of the samples taken, strain readings were recorded. The strain gages used were rectangular, three-element 45° rosette gages. The rosette gages allow for simultaneous measurement in three directions. The rosette gage is depicted in Figure 10.

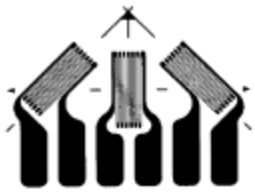

Figure 10. Rectangular, three element 45° rosette strain gage (After [7]).

Given the physical deformation transferred to a change in resistance reading, a measurement of strain can be recorded for each of the three elements. The strain transformation equations are the following [14]:

$$\varepsilon_1 = \frac{\varepsilon_x + \varepsilon_y}{2} + \frac{\varepsilon_x - \varepsilon_y}{2}\cos 2\theta_1 + \frac{1}{2}\gamma_{xy}\sin 2\theta_1$$

$$\varepsilon_2 = \frac{\varepsilon_x + \varepsilon_y}{2} - \frac{\varepsilon_x - \varepsilon_y}{2}\cos 2\theta_2 - \frac{1}{2}\gamma_{xy}\sin 2\theta_2$$

$$\varepsilon_3 = \frac{\varepsilon_x + \varepsilon_y}{2} + \frac{\varepsilon_x - \varepsilon_y}{2}\cos 2\theta_3 + \frac{1}{2}\gamma_{xy}\sin 2\theta_3$$

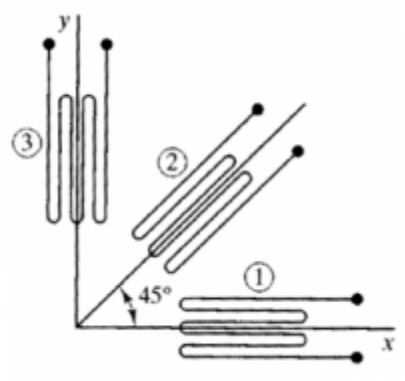

Figure 11. Rectangular rosette orientation (From [15]).

By using the orientation in Figure 11, thus setting $\theta_1=0°$, $\theta_2=45°$, $\theta_3=90°$, and assuming negligible shear in the xy plane for the vertical point load, the transformation equations simplify to the following:

$$\varepsilon_1 = \varepsilon_x$$

$$\varepsilon_3 = \varepsilon_y$$

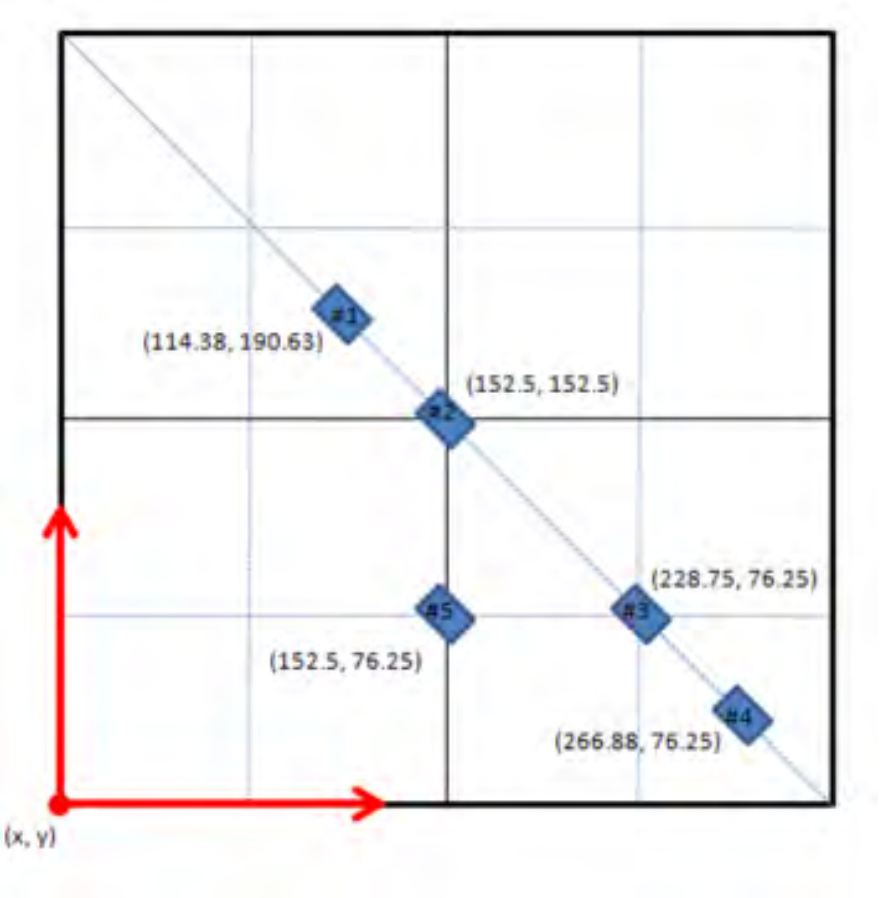

Figure 12. Strain gage layout.

A specific channel was assigned for the x and y strains as determined from the equations above and are given the assignments in Table 7.

Strain Channel	Gage #	Strain Direction
1	1	ε_y
3	1	ε_x
4	2	ε_y
6	2	ε_x
7	3	ε_y
9	3	ε_x
10	4	ε_y
12	4	ε_x
13	5	ε_y
15	5	ε_x

Table 7. Strain gage channels and directions.

The #2 gage at the center of the test area was not used for some tests in order to better allow for a better visual determination of the onset and growth of damage during progressive impact tests. The gages were bonded to the composite using a M-bond AE-10, in accordance with Vishay Precision Group Instruction Bulletin B-137 [16]. The gages were further waterproofed using a non-corrosive RTV sealant, 3140-RTV.

F. TEST EQUIPMENT

The test equipment used was the drop weight apparatus originally designed for the Owens study and subsequently used by McCrillis. As with the Owens and McCrillis experiments, the output of the impact test was a transient response of the sample for load and strain as a function of time.

1. Drop Weight Test Rig Apparatus

Owens describes the construction of the drop weight impactor in detail [7]. The impactor consisted of a drop weight and an impact rod supported by four steel guide rods and an aluminum frame base (Figure 13). The drop weight was guided by four linear bearings and a spring was used to eliminate the number of impacts during the drop. A

trigger (Figure 14) initiated the data acquisition discussed in paragraph II.F.2. The boundary conditions were simulated using eight (two per side) 76 mm (3 in) c-clamps. The drop weight could be fitted with additional free weights to vary the loads at a given drop height. The total impactor weight includes the impactor and the additional free weights added. The total impactor weights are detailed in Table 8. The drop height for the impactor could be varied. For this study, the drop heights ranged from 7.6 cm (3 in) to 76.2 cm (30 in). For the impactor weights used, a 76.2 cm drop height would typically be around the maximum load level for the load transducer.

Test Condition	Weight
Heavy Weight	10.84 kg
Medium Weight	8.75 kg
Low Weight	6.67 kg

Table 8. Varying weight test conditions for drop weight impactor

Figure 13. Dropweight test apparatus (From [7]).

Figure 14. Dropweight apparatus trigger mechanism.

2. Data Acquisition

The data acquisition system was also the same system developed for the Owens experiment [7,17]. The LabVIEW™ software was set to record at 10,000 Hz. The impactor recorded 1,000 samples over a 100 millisecond period when the trigger passed through the sensor pictured in Figure 14. Depending on the drop condition (weight, height), the ICP® force sensor manufactured by PCB Piezotronics, Inc, (Figure 15) would occasionally reach its maximum rated load of 4448 N (1000 lbf). Periodically, voltage spikes would cause maximum force and/or strain readings. These erroneous maximum values were manually removed from much of the data.

Figure 15. Force sensor.

3. Anechoic Tank

To minimize reverberation, an anechoic tank was used for the three test conditions: dry, submerged-water backed, and submerged-air backed. Tap water was the fluid medium used in the submerged cases. The tank is a 2.75 m cubic structure and a platform was used across the top of the tank to support the drop weight apparatus as it was lowered into the tank (Figure 16).

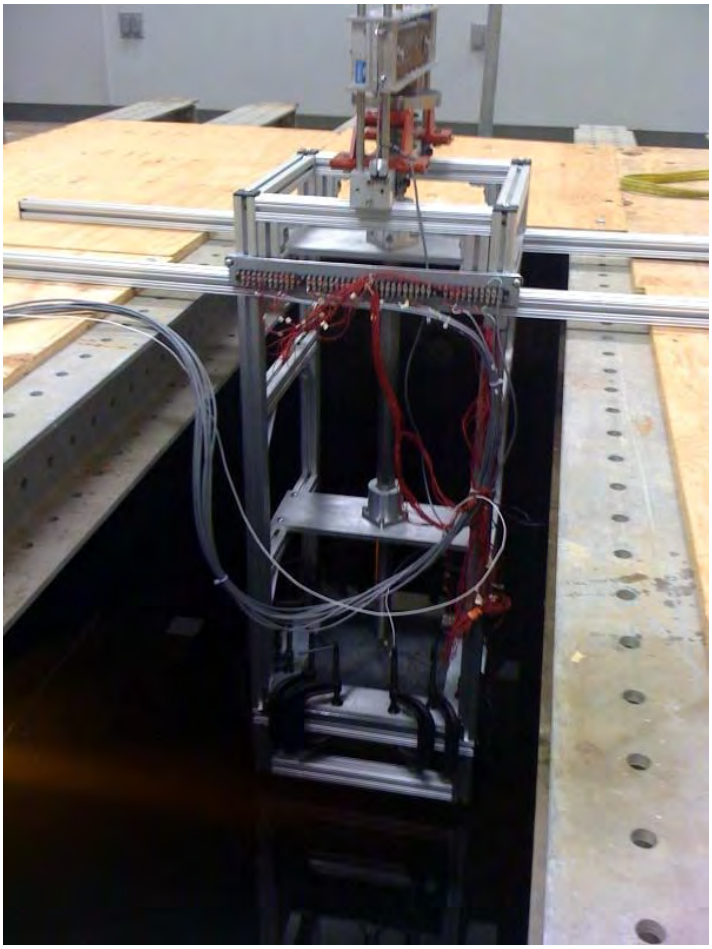

Figure 16. Drop weight testing apparatus in tank (From [7]).

III. TEST CONDITIONS

A. OVERVIEW

One of the primary goals of this study was to determine the composites behavior as the impact force was increased and to determine a point where the damage was first detected. Damage to many composites is often difficult to detect and there may be no observable reduction in mechanical properties until catastrophic failure occurs. For this reason, it is very important to understand the behavior of composites as the impact is increased until the onset of damage. It was for this reason that the 6.35-mm balsa core and ten skins of E-glass (five each side of the sandwich) were selected. There were other samples of various combinations that were also tested in order to determine the best composite for the study. In considering the multiple combinations, the 6.35mm/10-ply composite exhibited suitable strength characteristics at low impact force levels, but yet yielded adequate damage as the force levels were increased. Eleven of the thirteen analyzed samples were all of the 6.35 mm/10-ply construct.

B. TEST SAMPLE ENVIRONMENT

There were three basic environments in which the samples were tested.

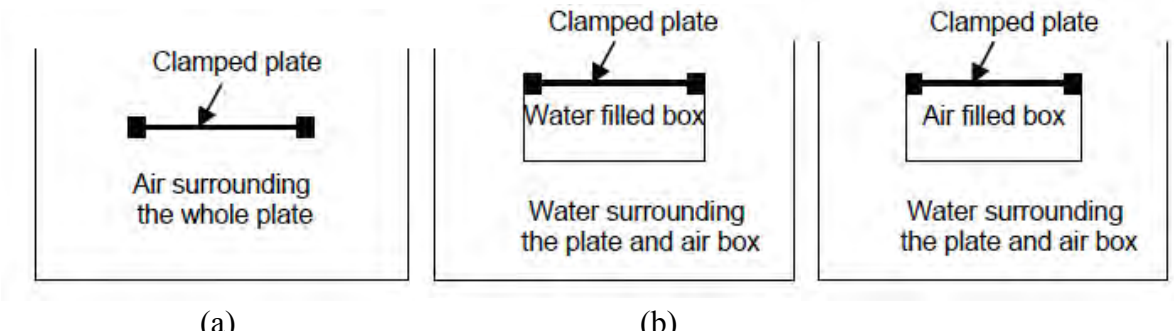

Figure 17. Three different impact conditions with composite plate held in place: (a) dry, (b) water backed, (c) air backed (After [17]).

1. Dry Impact

The dry impact condition was a baseline against other phases of testing. The drop weight impactor was lowered into the anechoic tank, and the water level was reduced well below the frame of the test apparatus.

2. Water Backed

The water-backed testing simulated a submerged object being impacted. Once the apparatus was lowered into the anechoic tank water level was raised well above the impact rod and test sample. As with the Owens study, the tank level was at least 50% of the plate length above the end of the impact rod. This minimized any disturbance level on the frequency response [7].

3. Air Backed

The tank was filled to the same level and the apparatus lowered in the same manner as the water-backed condition. The difference in this condition was a 330 x 330 x 127 mm deep plexi-glass box was affixed to the bottom of the test apparatus aluminum support plate. The 12.7-mm thick box was sealed to the test apparatus using the sealant tape and commercial "aquarium" sealant to prevent the intrusion of water into the box. The strain gage wiring harness was routed through a small hole in the box and then sealed with the aquarium sealant to prevent leakage.

C. DROP WEIGHT VARIATIONS

There were two different drop weights used in this study: 10.8 kg and 6.7 kg. The weights could be managed using a combination of specially manufactured free weight plates. The weights were varied for the variety of the test conditions in Paragraph B.

D. DROP HEIGHTS

The drop weights were dropped from a height of 7.62 cm (3 in) progressively to a maximum height of 76.2 cm (30 in). At the maximum drop height, it was in the range where the force sensor would reach its maximum recording levels. The drop height of 7.62 cm was low enough that for the samples tested incurred no damage. This was

important in evaluating the potential onset of damage for any sample. The initial two tests (Series 1) began at a drop height of 15.24 cm (6 in). Damage was immediately observed at the initial 15.24 cm drop for the water-backed sample, so the initial drop height was lowered to 7.62 cm to better ascertain the threshold for the onset of damage for the remaining samples.

E. OTHER TEST VARIATIONS

There was also a series of tests conducted with no balsa core within the composite. These tests were conducted to try and demonstrate similar composite responses while trying the eliminate some of the variations that occur naturally in the balsa wood. Two of the thirteen samples were tested in this fashion.

Sample	***Test Condition***	***Balsa Core***	***Drop Weight (kg)***	***Strain Gages***
Dry1	Dry	Y	10.8	N
Wet1	Water-Backed	Y	10.8	N
Dry2	Dry	Y	6.7	N
Wet2	Water-Backed	Y	6.7	N
Dry3	Dry	Y	10.8	Y
Wet3	Water-Backed	Y	10.8	Y
Dry4	Dry	Y	6.7	Y
Wet4	Water-Backed	Y	6.7	Y
Air4	Air - Backed	Y	6.7	Y
Dry5	Dry	N	10.8	Y
Wet5	Water-Backed	N	10.8	Y
Dry6	Dry	Y	6.7	N
Wet6	Water-Backed	Y	6.7	N

Table 9. Summary of test condition variation.

THIS PAGE INTENTIONALLY LEFT BLANK

IV. RESULTS AND ANALYSIS

A. OVERVIEW

One of the more challenging aspects of this study was getting consistent data to determine the fluid structure interaction on a sandwich composite. Specifically, that process was made more challenging using a core material as inhomogeneous as balsa wood. As mentioned earlier, the Pro Balsa Plus wood has been engineered to help reduce the inconsistencies in absorption of the resin during the infusion process; however, balsa wood is a naturally occurring material and has natural flaws that are typical of any piece of wood. Like a fingerprint, there are no two pieces of wood that exhibit the same characteristics, even in the same sample. The "butcher-block" appearance only exacerbates those differences.

There is some variation, or "scatter," in the data. However, through the testing and analysis of the thirteen samples, some distinct trends can be observed. While thirteen samples is perhaps enough to detect some general trends, the non-homogenous properties of composites and balsa wood in particular along with natural statistical variation lead to results with more "scatter" than desired.

The relative brittle nature of composites vs. metal structures is a key reason that the detection of damage is so important in composite structures [18]. There is a variety of damage characteristics for composite structures. In this study, the types of damage observed were almost exclusively delamination (Figures 20, 21, 22). The lone exception to the failure type was a penetration failure (Figure 22). However, it must be noted that the penetration occurred only after delamination had occurred, and after repeated impacts.

The added mass effect was observed when comparing the composite response in the differing fluid mediums. This effect was observed both experimentally in the force and strain responses of the various samples as well as analytically using the experimental natural frequency from the strain plots. Depending on the fluid medium in which the testing occurred, there was large variation in strain response at the same locations.

B. FORCE ANALYSIS

In the previous study by Owens it was found that her carbon-fiber plate had a density approximate to that of water. In this study, the balsa wood composite was much less dense. The balsa wood density was measured to be 606 kg/m^3, nearly 40% less than that of water. Due to this difference in density, as expected, there was generally a significant effect of water on the sandwich plate. One would expect then that the water would have a much larger impact on a less dense structure with the effect of Fluid-Structure Interaction (FSI). A complete summary of the force data for the thirteen progressive impact tests is detailed in Table 10.

Progressive Force Impact Data

	Drop Height (cm)																
*	*7.6*	*10.2*	*12.7*	*15.2*	*20.3*	*25.4*	*30.5*	*35.6*	*40.6*	*45.7*	*50.8*	*55.9*	*61.0*	*66.0*	*71.1*	*76.2*	*Damge Type*
Dry1	n/a	n/a	n/a	1888	2153	2723	2888	2937	2860	2867	3386	3557	3588	3499	4161	3909	Delamination
Wet1	n/a	n/a	n/a	1553	1725	2524	2694	2517	3095	3319	3331	3364	3765	4198	4198	4448	Delamination
Dry2	640	1041	-	1089	1191	1866	2028	2470	2473	2551	2871	2810	3014	3199	3250	2996	Delamination
Wet2	890	1052	1035	1113	1279	1391	1808	1856	2449	2189	2216	2722	2947	3249	2993	3706	Delamination
Dry3	771	945	1158	1153	1472	1689	2274	2295	2523	2641	-	949					Delam/Penetration
Wet3	703	1106	1171	-	1659	1961	2006	2036	2503	2584	-	2863	3152	3596	3528	3634	Delamination
Dry4	1228	1416	1297	1422	1614	1661	-	2690	2699	2896	3137	3332	3301	3653	3718	3716	Delamination
Wet4	792	934.2	1208	1473	1692	-	2440	2600	2743	2897	3275	3511	3664	3886	3900	4201	Delamination
Air4**	1022	1204	1429	1600	1663	1893	2062	2432	2574	2604	2708	3133	3069	3224	3345	3539	Delamination
Dry5	395	693	919	711	1245	1611	1951	2306	2882	3237	3545	3852	4164	4265	4145	4299	Delamination
Wet5	446.7	599	557	599	810	1297	1624	1973	2420	2727	2700	3295	3405	3573	3987	4009	delamination
Dry6	1120	1461	1748	2152	2336	2287	2902	3351	3674	3895	4044	4106	4286	max			Delamination
Wet6	788	1150	1364	1557	1852	2234	2471	2689	2923	3144	3144						Delam/Penetration
	3	*4*	*5*	*6*	*8*	*10*	*12*	*14*	*16*	*18*	*20*	*22*	*24*	*26*	*28*	*30*	
	Drop Height (in)																

*Forces in Newtons; '-' indicates test error; shaded cells indicate onset of damage
** Onset of damage cannot be determined due to air box structure around composite

Table 10. Progressive force impact data.

In reviewing Table 10, the best comparisons can be observed for the samples with matching post-scripts series numbers. For example, Dry1 and Wet1 samples were conducted at approximately the same time and with samples of the same relative age insofar as their postcuring shelf life. It should be noted that there was no noticeable differences in composite performances based on shelf life as the period of manufacturing and testing was condensed to less than six months. Perhaps this variable would produce some noticeable variation over a longer period of time.

While the observed force levels may indicate a lower force level for the wet impact at the same drop height (792 N (wet) vs 1228 N (dry) as an extreme example), what must be considered is any loss of stiffness in a damaged sample. Intuitively, it can be shown that as stiffness increases the force on an object will be much greater. Think of a billiard ball being dropped on a steel plate versus dropped on a rubber mat. The (lack of) stiffness absorbs the force of the ball and as a result a force reading would be much lower for the rubber mat example. The same analogy can be applied to the impact test on the composite sandwich. Any damage to the composite would produce a less stiff member and thus lower force levels. This is but one factor that can explain a lower force reading at the same drop height. Perhaps just as significant is the lack of isotropic material. Composites by nature have large variations in material properties due to fiber alignment and placement, differences in resin absorption, and in the case of balsa wood, large variations in the core material. An empirical test does not need to be conducted to know there are large variations in the balsa wood. A visual inspection of the material reveals large variations in density from the dark to light sections. In addition, the seams of the balsa "butcher block" can also be a point where there would be large variations in the material property.

Even with the larger force level for the dry vs. water-backed sample for Dry4 and Wet4, the water-backed sample suffered damage at a lower drop height than dry sample. In every case when the samples within a series are compared, the onset of damage occurred earlier in the water-backed vs. dry samples for samples of the same series. While the E-glass laminate was selected to help discern the very onset of damage, there may be some initial internal damage that could not be detected and contributes to the lower force level reading. Additionally, a look at the strain data for the same samples (Figure 18) in the y-direction show nearly double the deformation for the Wet4 vs Dry4 samples.

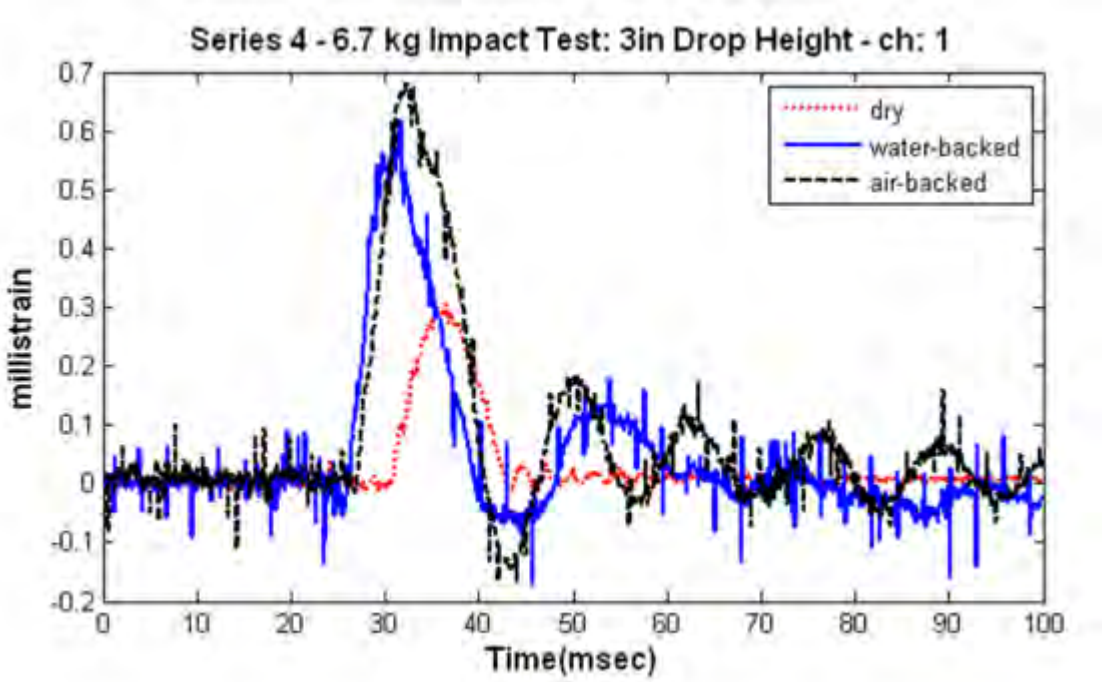

Figure 18. Strain deformation. Series 4, ε_y at Gage #1 (114.38, 190.63) mm.

A further study of strain response will occur in the subsequent section, but Figure 18 is used to highlight an applicable, simplified one degree of freedom view of stiffness. Stiffness (k) is inversely proportional to the deformation (δ), by the equation:

$$k = F/\delta$$

From this, one can see that the larger deformation will yield a lower stiffness for the same force (F) level. Since the force response is being recorded from the composite onto the sensor the ability to "push-back" is greatly reduced and thus yields a much lower force level observed in the study.

For the samples in series 1 and 2, prior to placing strain gages on the sample, the composite was able to be removed after each progressive drop to capture a photograph of the delamination growth (if any). Figures 19 and 20 show the Dry1 and Wet1 sample at an identical drop height. The water-structure interaction vs. the air-structure interaction is clearly evident through the added mass effect of the water on the less dense composite.

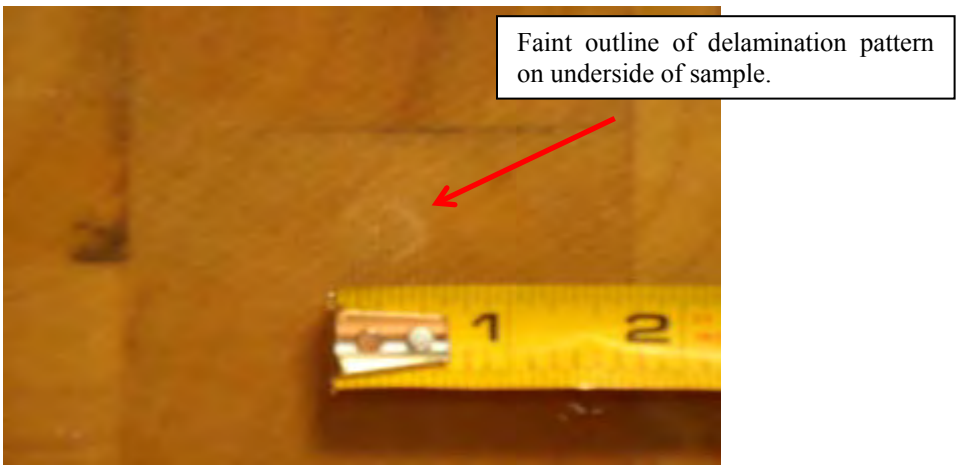

Figure 19. Sample Dry1 at 14” drop height.

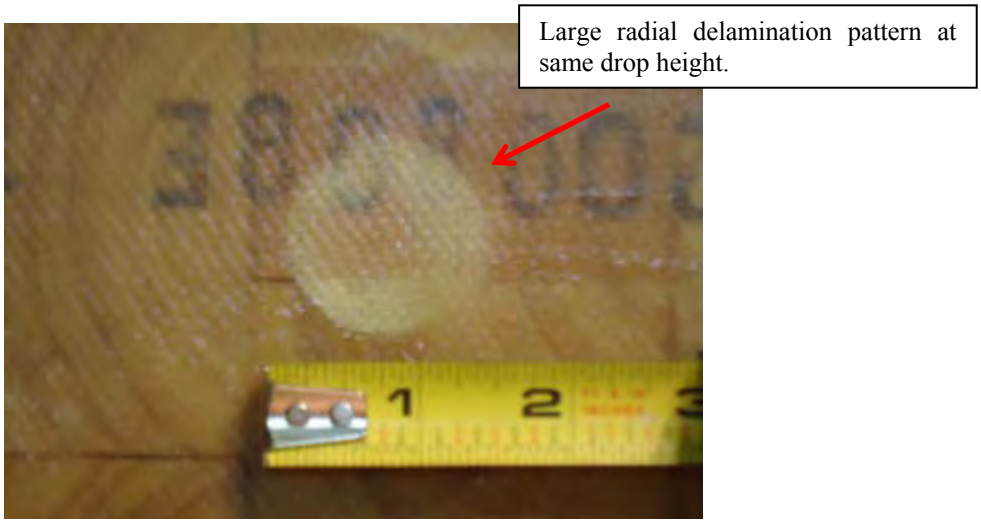

Figure 20. Sample Wet1 at same 14” drop height.

A closer look at the series 1 tests show the above added mass effect in water as well as the reasoning for lowering the initial drop height to 3 in. Table 10 shows the initial force level of 1,888 N (dry) vs. 1,553 N (water backed) for samples Dry1 and Wet1 respectively. Table 10 also shows the initiation of damage upon first impact at this drop height for the water-backed sample. With the increased deformation and the reduced stiffness from the damage, the force levels were subsequently lower for the water-backed sample. Lowering the initial drop height allowed for some measurements

prior to the onset of damage. The damaged sample only intensifies the non-homogenous properties between samples. Thus, comparing a damaged sample with an undamaged sample does not allow for a "fair" comparison. There was no observed damage from a drop any lower than six inches with the visual techniques used in this study. As suggested above, this is not to say that there was not internal damage between the laminate skins and/or the core before impact. The lower force levels coupled with the observed delamination at a lower drop height suggest the onset of damage may actually occur before any visual indication.

Figure 21. Sample Wet1 initial damage at 6 in drop height.

An example of penetration failure is shown in Figure 22 for Sample Dry3. The failure due to penetration is due to the cellular matrix breakdown after repeated impacts at the same location.

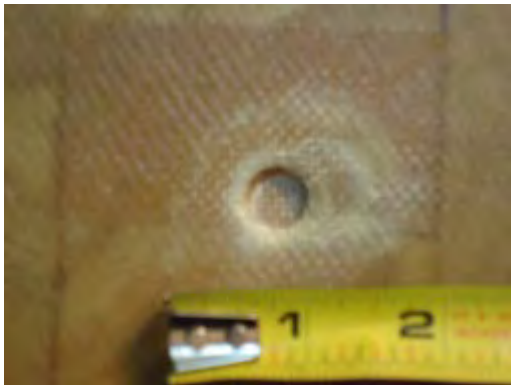

Figure 22. Sample Dry3 penetration failure.

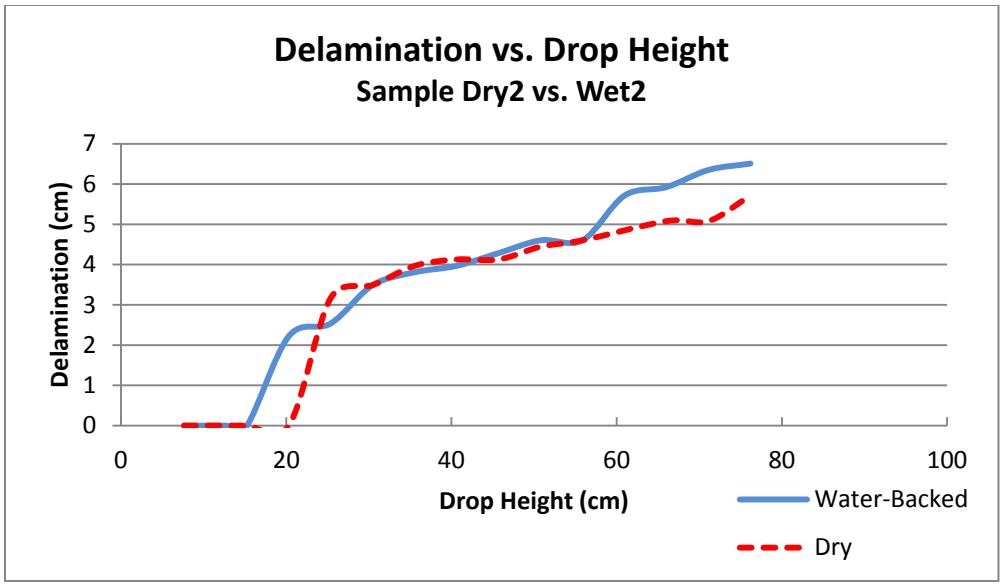

Figure 23. Delamination occurs earlier and generally is more widespread when the added mass effect is more prevalent.

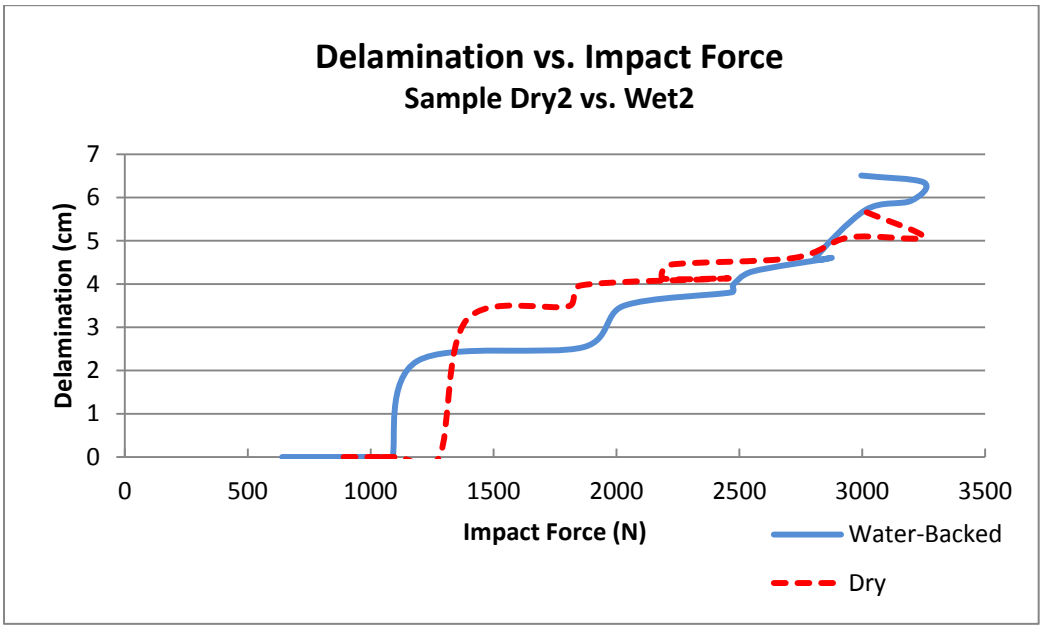

Figure 24. Delamination vs. impact force. Typically damage occurs first for water-backed sample and then a "crossing" occurs where we can expect to see higher delamination for the same impact force in a dry sample.

	WATER-BACKED (cm)		DRY (cm)	% Diff
Wet1	6.4	**Dry1**	4.5	+30%
Wet2	6.5	**Dry2**	5.7	+12%
Wet3	Delam not discernable due to strain gage surface prep	**Dry3**	Delam not discernable due to strain gage surface prep	
Wet4	5.7	**Dry4**	5.9	-3%
Wet5	2.9	**Dry5**	2.5	+14%
Wet6	5.1	**Dry6**	4.8	+6.3%

Table 11. Total delamination damage diameters. Green "+" indicates % gain for water-backed FSI.

In the series 5 tests, when the balsa core was removed, the hope of the study was to eliminate the large variation in structural properties as with the balsa wood. Like the previous samples, the dry sample demonstrated consistently higher force levels. Also like the previous samples, the failure of the water-backed sample occurred at a lower drop height than the dry case. For these two samples the delamination failure occurred at a significantly higher force level than the balsa core samples, nearly 2–2.5 times higher in magnitude. The ability for the skin layers to better adhere to like materials explains the higher threshold, as delamination is likely to occur at an interface. The likelihood for the disbonding to occur between two different materials with different fibrous orientations is greater between E-glass and balsa wood than two sheets of E-glass.

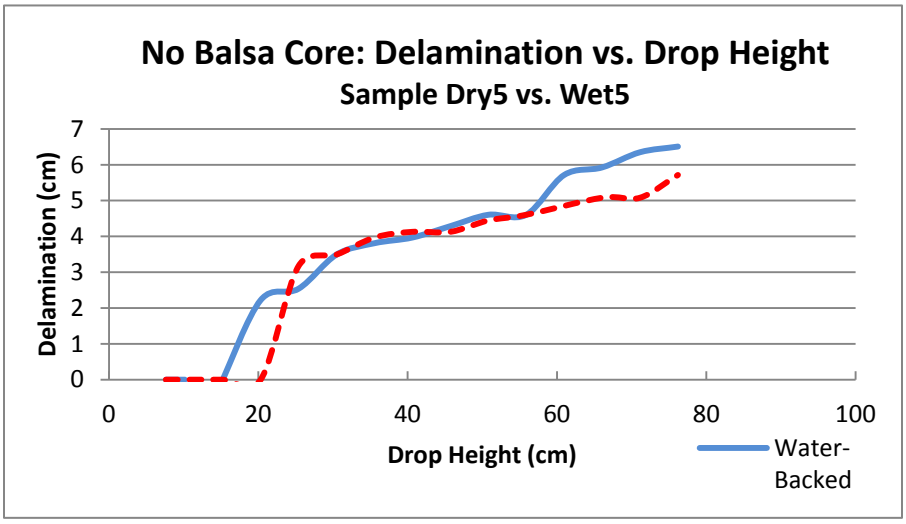

Figure 25. Delamination vs. drop height: No balsa core. Again, the added mass effect.

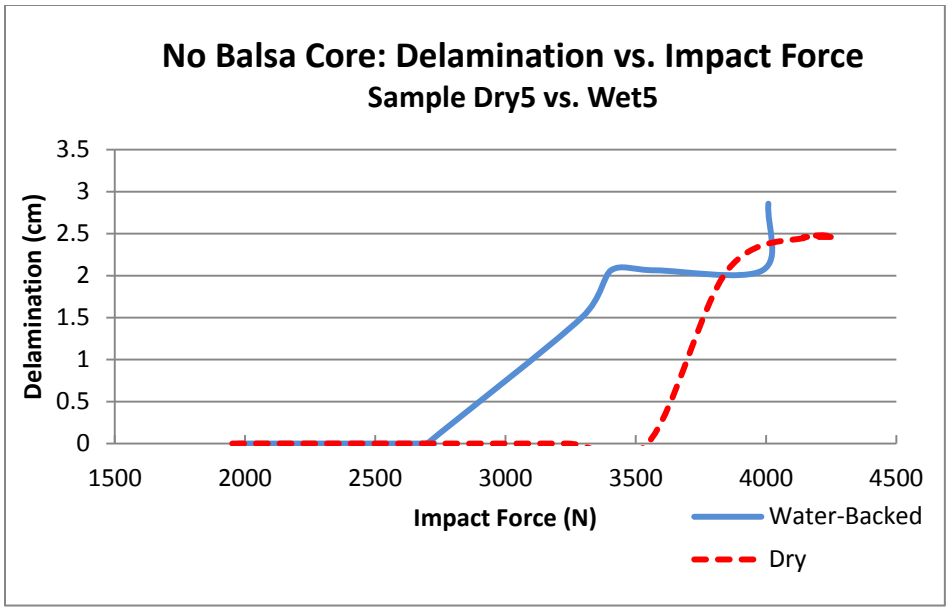

Figure 26. Delamination vs. impact force: No-core composite. The same "crossing" of the dry and water-backed sample. This time for a shorter duration due to the delay in the onset of damage for the non-core sample.

An examination of Table 10 and a close look at impact force levels raises the question as to why the impact force for the 6.7 kg lower weight impact is generally higher in the series 4 and series 6 tests than for the 10.8 kg series tests. There are a couple of sources of error or inconsistencies that could lead to these results. As previously mentioned, the impactor may strike a more dense location of the balsa wood that would be more stiff than an adjacent less dense section of the balsa. Additionally, error from the test rig itself is a possible source of error. Efforts were made to maintain a constant clearance between the impactor and the sample for all tests. However, just due to the nature of the construction of the test rig may allow for some variation in this clearance. A sample that was impacted with more clearance to the sensor, would have more if the impact energy absorbed by the rig's spring prior to sample impact and thus a lower force level recorded. The combination of these two factors likely contribute to a significant portion of the scatter of force level data.

There has been a great effort devoted in this section in explaining why there might be a lower force level for a water-backed sample. If one is to make the argument that

there is an added mass effect due to the water's relative density to the sandwich composite, then this result seems somewhat counter intuitive. After all, the wide scattering of force levels between wet/dry, light/heavy weight samples is significant. A couple of different ideas on that phenomenon are explained in relative stiffness, damage, and inconsistency in the composite and test rig itself. However, the only true test in comparing the fluid structure interaction in various medium is to use the same sample. The series 4 samples sought to accomplish this. The weight of the impactor was lowered to 6.7 kg and the sample was tested under dry, water-backed, and air-backed conditions at a drop height of 3 in. By lowering the drop weight and using the lowest drop level, one can reasonably assume based on the composite performance to date that the sample would not suffer any damage. In doing this, the variables mentioned previously could be nearly eliminated and a "fair" comparison could be conducted. In terms of force, there was a 16.3% higher force level recorded for the water-backed sample than that of the dry sample. The air-backed wet impact sample was nearly identical in terms of magnitude to the dry sample. The fluid structure interaction produced three completely different force shapes. The wet impact samples peaked earlier than the dry sample and had multiple peaks. The air-backed sample had multiple, nearly identical magnitude peaks, while the second water-backed peak was more modest. The strain deformations also support the added mass effect from the water-backed samples and will be discussed further in the next section. With all conditions being kept as equal as possible, the added mass effect is clearly demonstrated for the water-backed case.

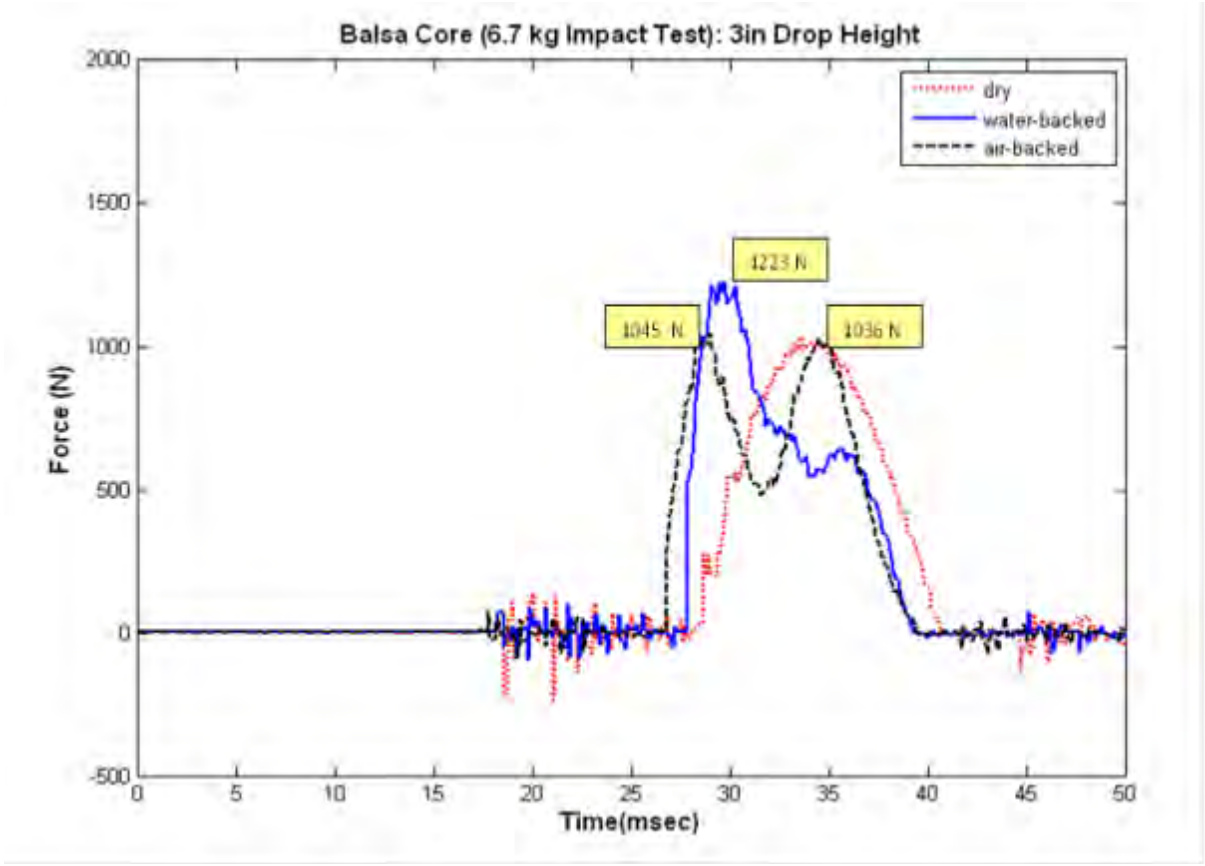

Figure 27. A clear indication of the presence of the added mass effect with the composite samples on a "level playing field."

C. STRAIN ANALYSIS

As shown earlier, the strain performance can give significant insight into the fluid structure interaction and is perhaps the most direct method used in this study. For an identical drop height in conditions aimed to mirror each sample as much as possible, the deformation of the sample can give very direct clues into the sandwich composite's performance. In general, the study shows that the wet impact water-backed samples displayed the largest strain deformations at each gage location. The lone exception was gage #1 which had the closest magnitudes for each of the test conditions, with the dry sample having a much higher magnitude for the non-balsa core samples of series 5. For each test, the maximum strain values varied at gage #1. Figures 29 through 38 will give a

representative sampling of both the ε_y and ε_x data for each gage. In terms of magnitude of strain and frequency response it is clear that an added mass effect is present for the fluid structure interaction in water.

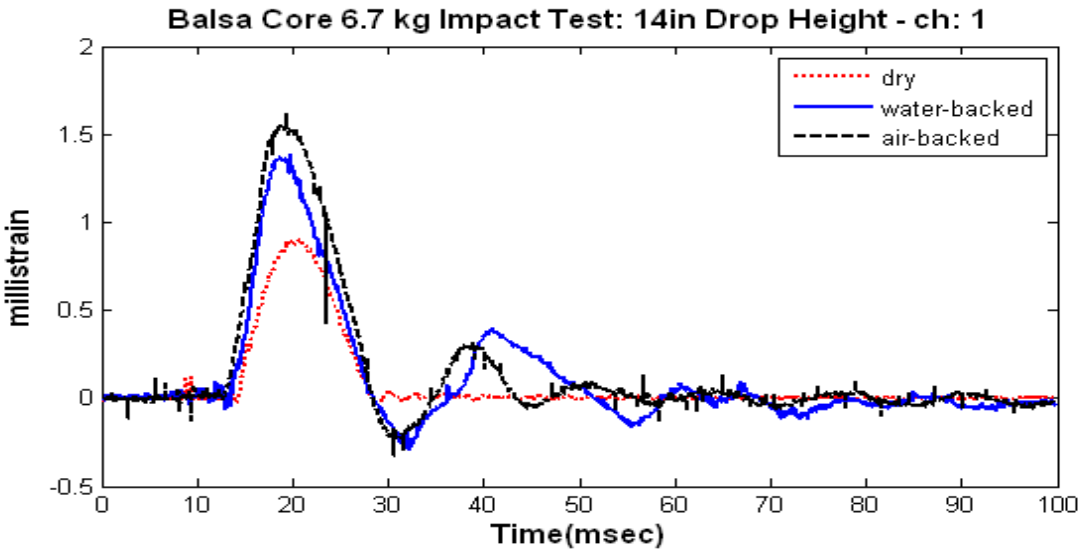

Figure 28. Representative ε_y gage 1 response. One of the few gage responses where the maximum magnitude was not that of the water-backed sample.

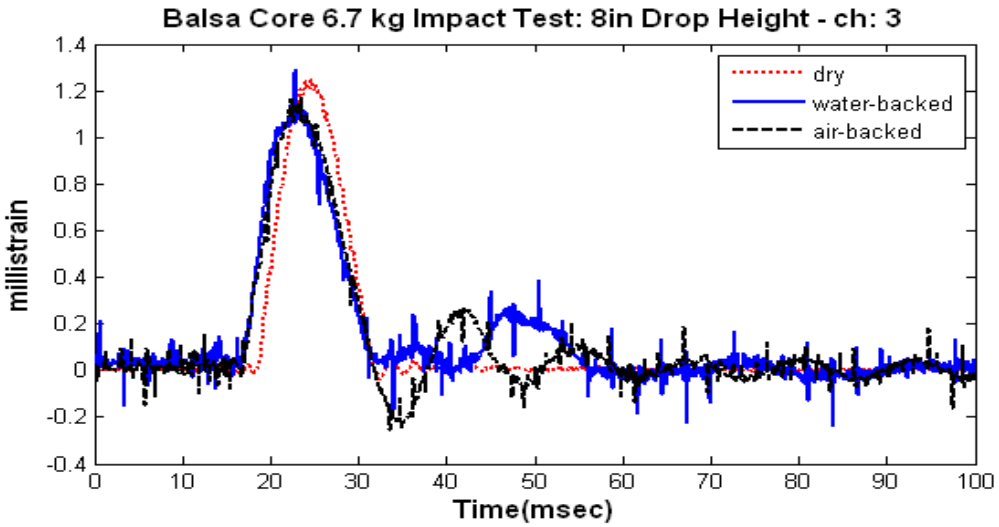

Figure 29. Representative ε_x gage 1 response. Another example of the wide scatter of data that was observed at gage location 1. This is one of the only locations where the dry sample was observed with the maximum magnitude.

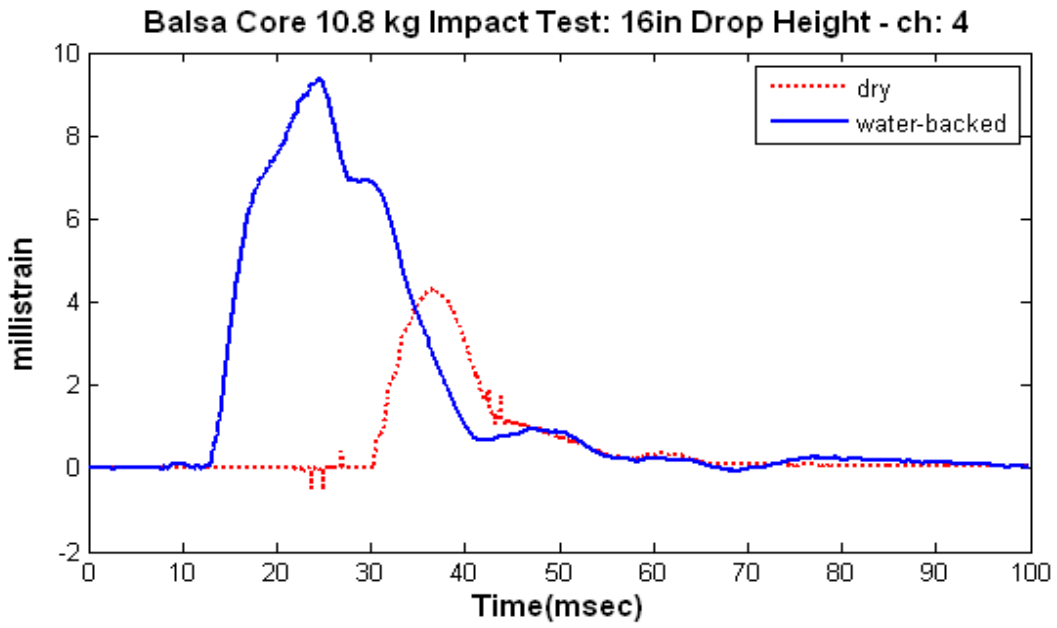

Figure 30. Representative ε_y gage 2 response. Directly under impact.

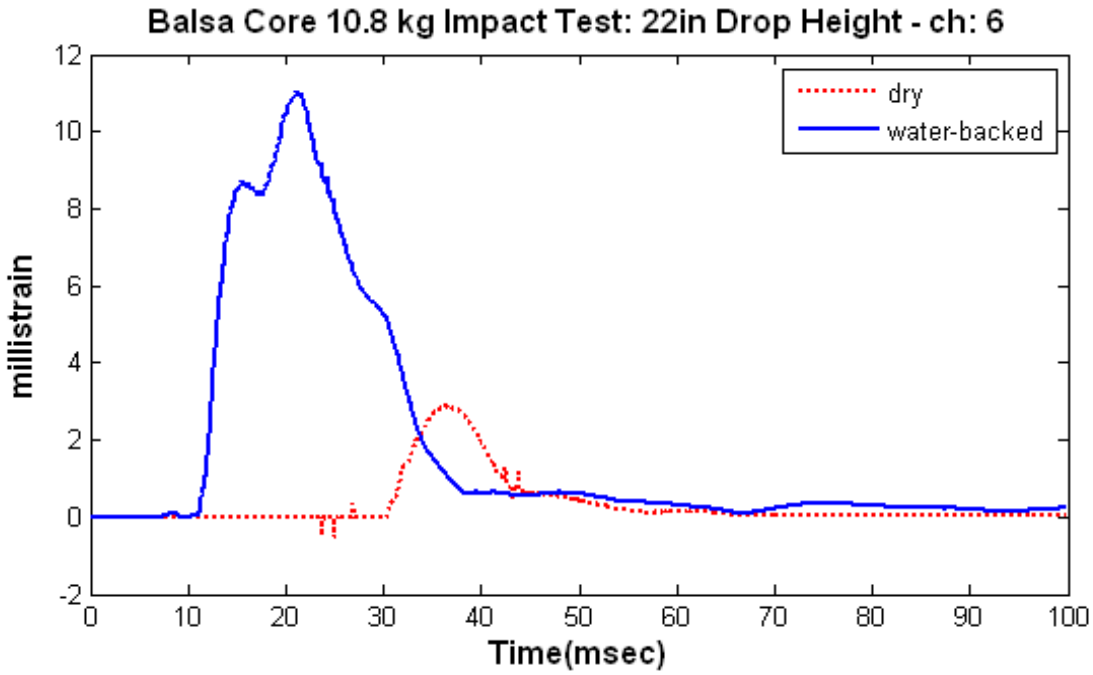

Figure 31. Representative ε_x gage 2 response. Again directly under impact.

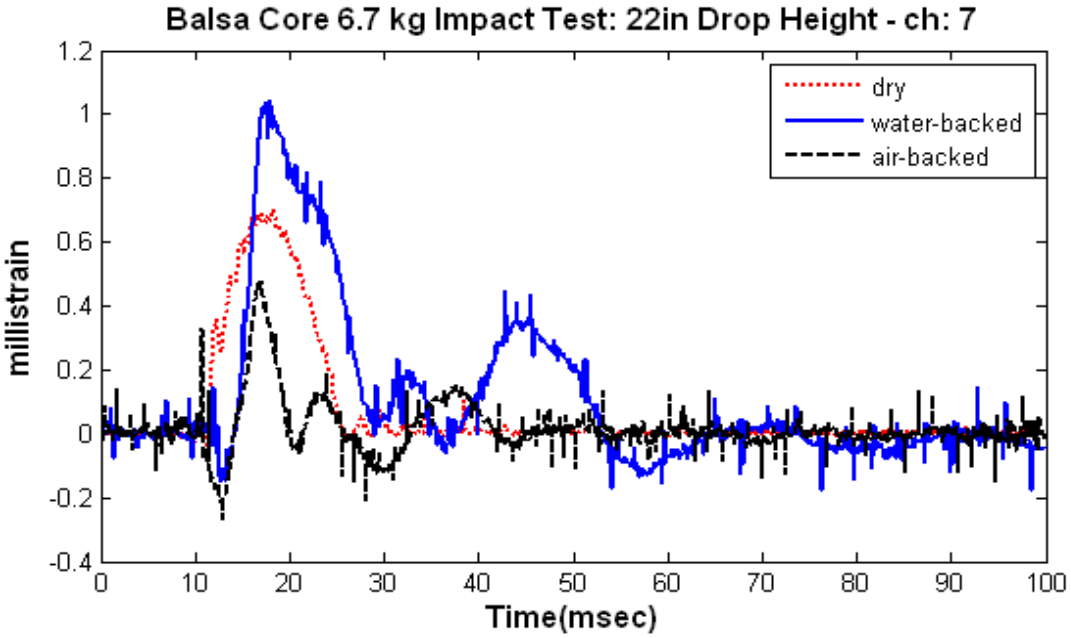

Figure 32. Representative ε_y gage 3 response.

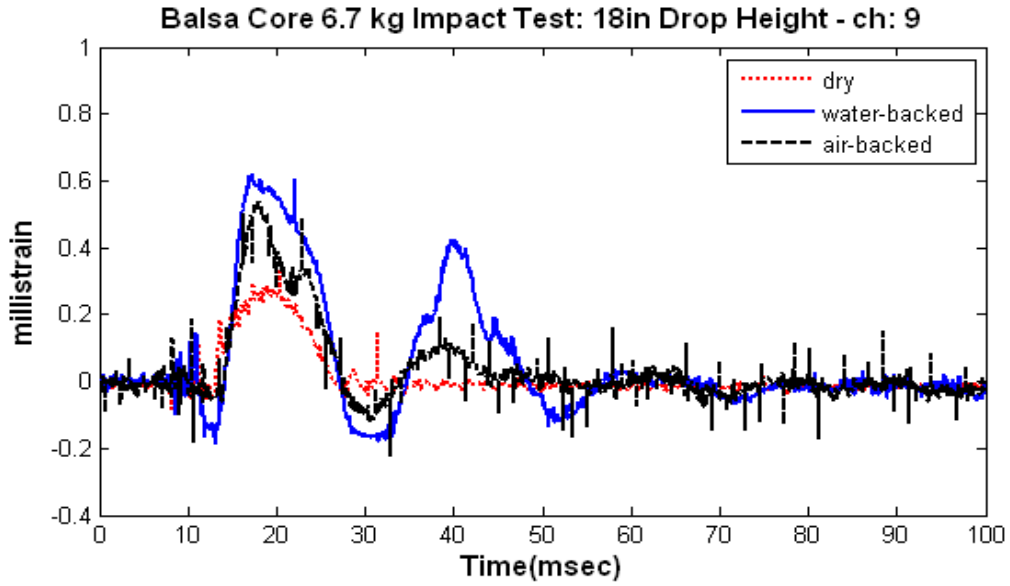

Figure 33. Representative ε_x gage 3 response. The damping ratios for the air and water backed are similar.

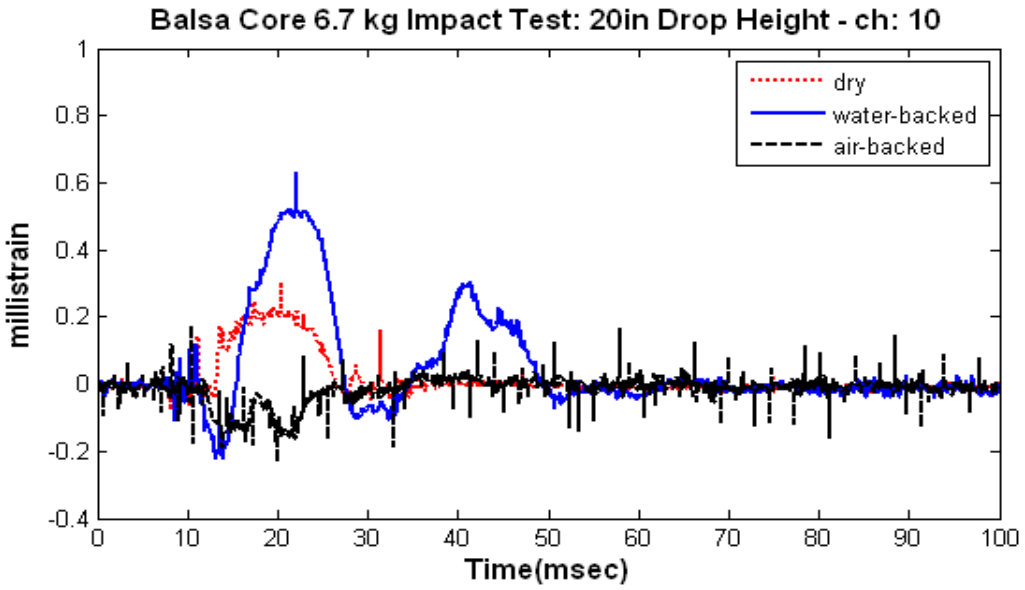

Figure 34. Representative ε_y gage 4 response. As the gage is positioned nearer the clamped boundary conditions we begin to see large variation in response. While two samples are in tension the other in compression; suggestive that not only the natural frequencies, but the mode shapes are entirely different based on the medium.

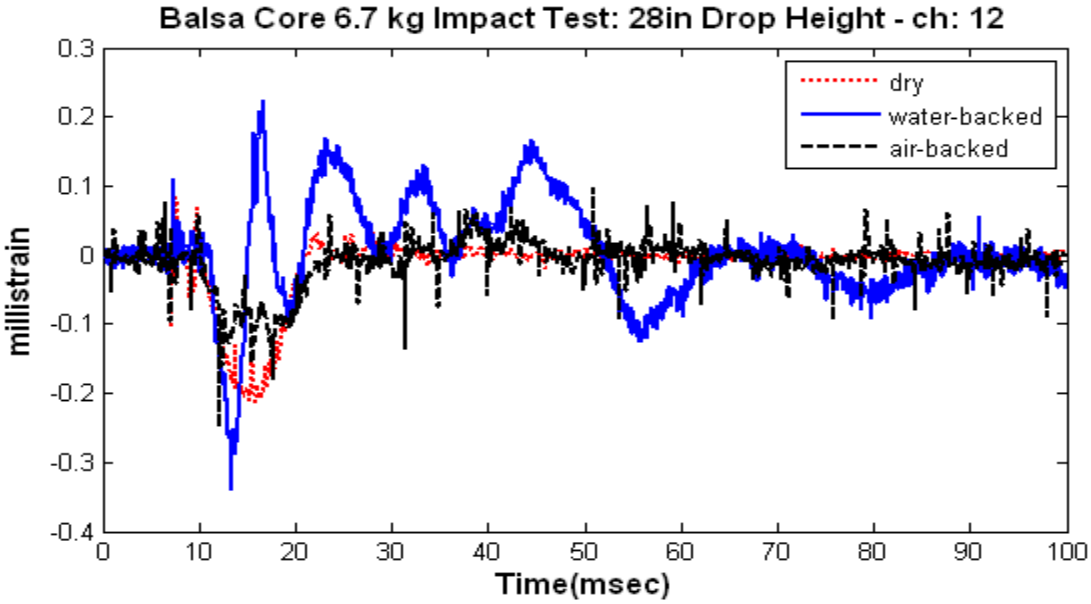

Figure 35. Representative ε_x gage 4 response. The same erratic behavior at the boundary conditions.

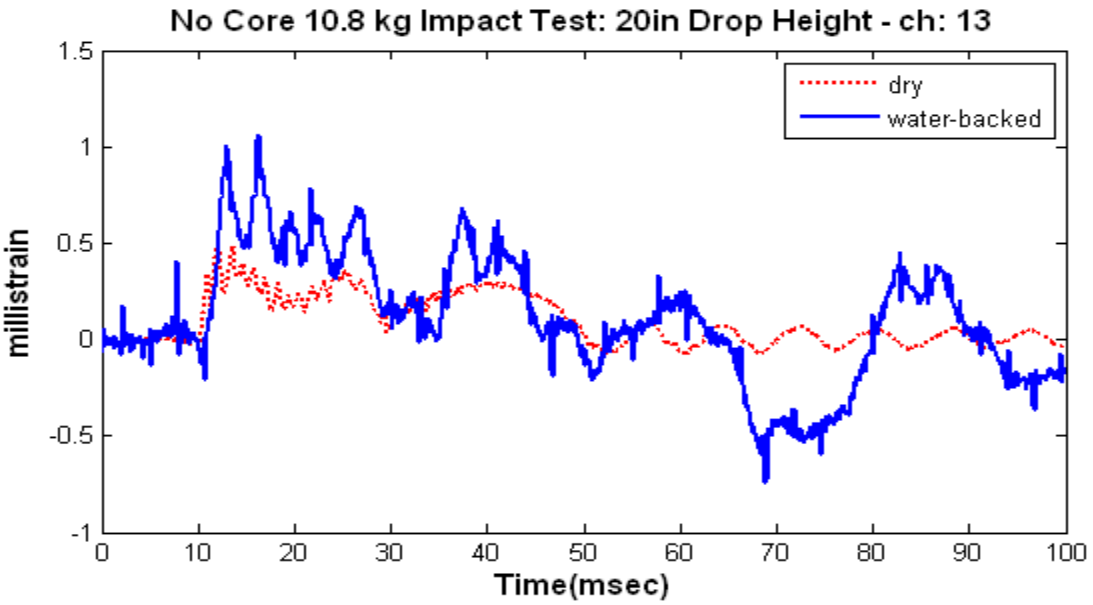

Figure 36. Representative ε_y gage 5 response. Generally consistent throughout, the water-backed samples have the largest strain magnitude.

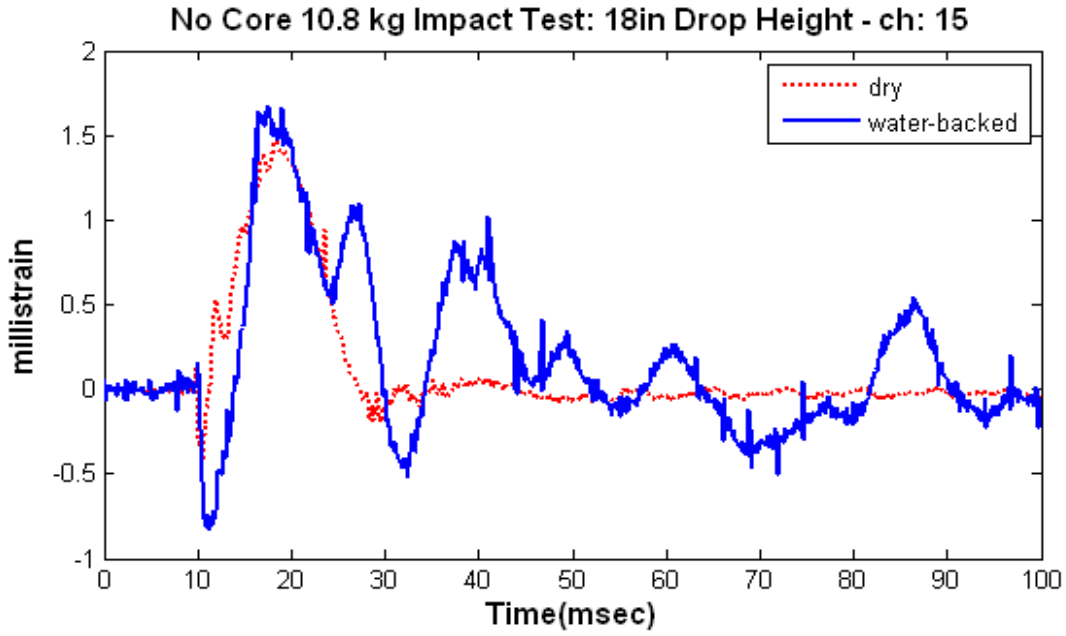

Figure 37. Representative ε_y gage 5 response. The water-backed sample is consistently damped slower than the dry samples.

In addition to the magnitude we can make some analytical analysis to demonstrate the added mass effect through the natural frequency of the sample during impact. It was somewhat difficult to find a strain response with a regular oscillatory pattern, particularly for the dry samples. Using the method below, as with the Owens study, gages #3 (228.75, 76.25) mm and #5 (152.5, 76.25) mm were selected for their somewhat regular oscillatory pattern. The first peak at the point of free vibration after probe impact (the largest magnitude strain reading) was used for both the dry and water-backed samples.

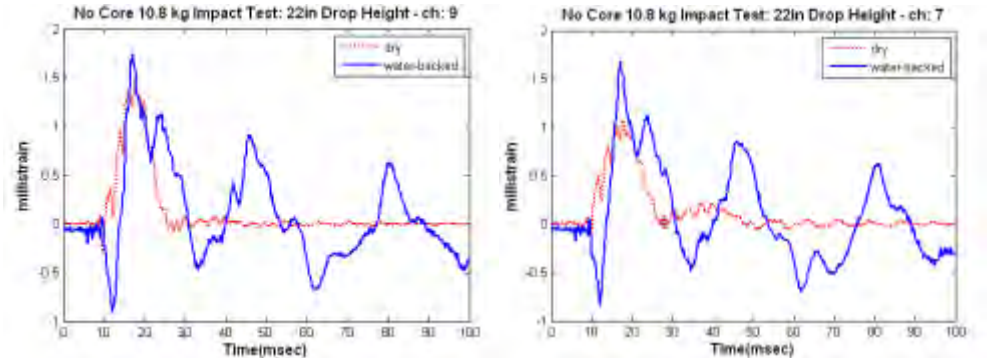

Figure 38. Strain plots (ε_x and ε_y) for gage #3.

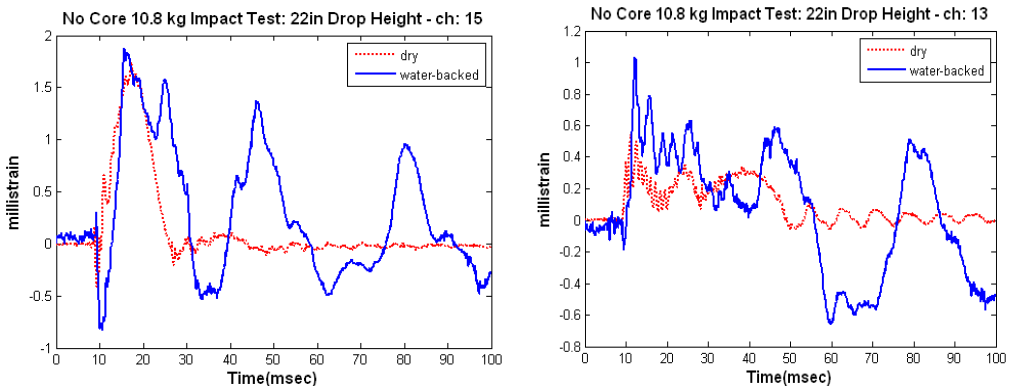

Figure 39. Strain plots (ε_x and ε_y) for gage #5.

Using the same method described by Owens to determine natural frequency, the following table details critical calculations in leading to the natural frequency of the composite plate under varying test conditions.

	Period	Damped Nat Freq	Damping Ratio	Natural Freq
Gage 3	**T (sec)**	**ω_d (rad/sec)**		**ω_n (rad/sec**
Dry - ε_x	0.012	532.5	0.053	533.2
Wet - ε_x	0.035	180.0	0.059	180.3
Dry - ε_y	0.010	637.2	0.060	638.4
Wet- ε_y	0.035	180.0	0.051	180.3
Gage 5				
Dry - ε_x	0.011	573.8	0.219	588.1
Wet - ε_x	0.034	184.3	0.057	184.6
Dry - ε_y	0.0099	634.7	0.044	635.3
Wet- ε_y	0.033	190.4	0.025	190.5

Table 12. Representative natural frequencies for the non-core sample.

From the natural frequency calculations, the added mass factor (AMF), $\beta = m^*/m$, can be obtained from Haddara and Cao's study [19].

$$\omega_{(wet)} = \omega_{(air)} * (1/(1+m^*/m)^{1/2})$$

In this case, the ωf is the natural frequency of the water-backed wet impact and the ωair is the dry samples. Using this relationship the AMFs are tabulated below for the representative sample.

Gage 3	**AMF, β**
Wet - ε_x	7.74
Wet- ε_y	11.5
Gage 5	
Wet - ε_x	9.15
Wet- ε_y	10.1

Table 13. Added Mass Factors (β).

From Figures 38 and 39, it is clear, particularly in the x strain, that the oscillations of the dry samples become damped very quickly when compared to the wet samples. While the exact amplitudes and periods may be difficult to discern exactly on the graphs given the variation in some of the data, a "quick-look" at the large difference in frequency response and an understanding of the relationship of the natural frequencies to

the dimensionless AMFs will prove a clear added mass effect in the water. The average AMF for this small sample was 9.6. The added mass effect was experimentally found to be a 16.3% increase when the same sample was tested under identical conditions. While there may be some variation in these numbers, the qualitative observation is clear.

In the Owens study, calculated natural frequencies, yielded an average AMF of 6.6 for her carbon-fiber composite. Published AMF factors for steel are shown to range from 1.4 to 2.4 depending on the boundary conditions [7]. Despite a relatively small sample size, the higher AMF for the balsa wood sandwich composites is consistent with the trend that as density decreases, AMF will increase and the fluid-structure interaction more prevalent.

With only one sample in the air-backed condition one cannot identify a clear trend. However, the data that was gathered does seem to support a similar response to that of the water-backed in terms of both magnitude and frequency response. The air-backed sample appears to be less damped than the dry sample and would subsequently also show an AMF. From the minimal sampling on the air-backed case it would appear that the AMF would be something less than what was observed for the water-backed case.

THIS PAGE INTENTIONALLY LEFT BLANK

V. CONCLUSIONS

This study sought to build upon the work of fluid-structure interactions to better understand the dynamic response of a sandwich composite. The results concluded that the added mass effect of the fluid structure interaction plays a significant factor in the response of a sandwich composite, both in terms of force and frequency response.

The major findings of this study show that the dynamic response varies depending on the fluid in which the test was conducted. Specifically, as the test medium becomes more dense (water vs. air), there is an added mass effect that effects the dynamic response of the sandwich composite. The added mass effect of the fluid-structure interaction is intensified as the densities of the composite are lowered below that of the density of water. Analytically this is observed as the AMFs were highest for the lower density balsa-core sandwich composites. As the density decreased, this study showed an increase AMF over previously studied carbon fiber composites [7, 17] and published reports of steel fluid-structure interactions [7].

Experimentally, this study showed clear trends indicating an increasing effect of the fluid-structure interactions in water vs. air. For each series of tests, it was conclusive that the damage occurred at a lower drop height because of the added mass effect. In addition to the earlier onset of damage, the delamination patterns were generally larger at every drop height for the water-backed samples when compared to the dry baseline. The dynamic response demonstrated through the magnitude of the strain deformations, showed a clear trend that the water-backed impact, was producing larger strains in almost every location.

This study also found through an investigation of the strain response, particularly near the boundary conditions, that the frequency responses were different not only in terms of magnitude, but also in modal shapes. For design considerations, this study highlights the need to specifically test composites in their intended operational fluid medium in order to properly determine natural frequencies.

Including FSI effect for a composite structure in contact with water is essential for the structural design and analysis. Otherwise, the analysis would be nonconservative.

VI. RECOMMENDED FURTHER STUDY

The trend in the military marine industry to expand its use of composites will continue thus it is recommended that further study be conducted to continue this work. Of particular interest, is the submerged air-backed model. This model perhaps best represents that of a submerged hull form. Since the use of composites in critical combat structures in U.S. Navy applications is relatively young and growing, the effect (if any) or the post curing process should be studied further. Gathering this information on composite performance over time may help ships to meet or exceed expected service life expectations. It will be very beneficial to measure the full field deformation and compare it between the dry and wet impact cases. Additionally, it is recommended that the experimental data be compared with the computational results to better understand the FSI effect on composite structures.

THIS PAGE INTENTIONALLY LEFT BLANK

LIST OF REFERENCES

[1] J. R. Vinson and R. L. Sierakowski, *The Behavior of Structures Composed of Composite Materials*. Secaucus, NJ: Kluwer Academic Publishers, 2002.

[2] NASA Preferred Reliability Practices: Structural Laminate Composites for Space Applications, Practice No. PD-ED-1217, NASA Jet Propulsion Laboratory California Institute of Technology, 2009, http://engineer.jpl.nasa.gov/practices/1217.pdf. Accessed August 24, 2010.

[3] Business Development in the New Navy, Ball Aerospace & Technologies Corp, Boulder, CO, August 2003, http://www.nps.edu/academics/institutes/meyer/docs/SI4000/Seminar_topics_04/Navy_Marketing_Brief_Ball_Aerospace.pdf. Accessed August 24, 2010.

[4] M.R. LeGault, "DDG-1000 Zumwalt: Stealth Warship," *Composites Technology*, February 2010.

[5] B. Griffiths, "Rudder gets new twist with composites," *Composites Technology*, August 2006.

[6] S. Abrate, *Impact on Composite Structures*. United Kingdom: Cambridge University Press, 1998.

[7] A.C. Owens, "An Experimental Study of Fluid Structure Interaction of Carbon Composites Under Low Velocity Impact," M.S. thesis, Mech. Eng., Naval Postgraduate School, Monterey, CA, 2009.

[8] R.D. McCrillis, "Dynamic Failure of Sandwich Beams with Fluid Structure Interaction Under Impact Loading," M.S. thesis, Mech. Eng., Naval Postgraduate School, Monterey, CA, 2010.

[9] DIAB Sandwich Handbook: Sandwich Concept, DIAB AB, box 201, S-312 22, Laholm, Sweden, September 2003, http://www.diabgroup.com/europe/literature/e_pdf_files/man_pdf/sandwich_hb.pdf. Accessed August 23, 2010.

[10] U.S. Composites Woven Cloth Product Information, http://www.uscomposites.com/cloth.html. Accessed August 24, 2010.

[11] Derakane 510A-40 Epoxy Vinyl Ester Resin Technical Data Sheet, Ashland Composite Polymers, Columbus, OH, November 2004, http://www.derakane.com/downloadServlet?docPath=DPAPP1.asco.ashland.com%5CData%5Cascc%5Cecomdocsasc.nsf%5C9E5FEE992B7A2EEC85256F78005B1367%5C%24FILE%5C510A-40.pdf. Accessed August 24, 2010.

[12] Derakane 510A-40 Epoxy Vinyl Ester Resin, Typical Gel Times Using MEKP, Ashland Composite Polymers, Columbus, OH, November 2004, http://www.derakane.com/derakaneControllerAction.do?method=goToGelTimePage&actionForwardName=510A40GelTimePage1. Accessed August 24, 2010.

[13] P. K. Mallick, *Composites Engineering Handbook*. New York: Marcel Dekker, 1997.

[14] A. C Ugural and S. K. Fenster, *Advanced Strength and Applied Elasticity.* Upper Saddle, NJ: Prentice Hall Professional Technical Reference, 2003.

[15] I. H. Shames and J. M. Pitarresi, *Introduction to Solid Mechanics*. Upper Saddle NJ: Prentice Hall, 2000.

[16] Vishay Precision Group: Instruction Bulletin B-137: Strain Gage Applications with M-Bond AE-10, AE-15 and GA-2 Adhesive System, Vishay Precision Group 3, Malvern, PA, March 2010.

[17] Y. W Kwon, A. C. Owens, A. S. Kwon, and J. M. Didoszak, "Experimental study of impact on composite plates with fluid-structure interaction." *The International Journal of Multiphysics*, vol. 4, no. 3, 2010.

[18] T.J. Reinhart, *Engineered Materials Handbook, Volume 1, Composites.* Metals Park, OH: ASM International, 1987.

[19] M.R. Haddara and S. Cao, "A study of the dynamic response of submerged rectangular flat plates," *Marine Structures*, March 1996.

INITIAL DISTRIBUTION LIST

1. Defense Technical Information Center
   Ft. Belvoir, Virginia

2. Dudley Knox Library
   Naval Postgraduate School
   Monterey, California

3. Distinguished Professor Young Kwon
   Naval Postgraduate School
   Monterey, California

4. Research Assistant Professor Jarema M. Didoszak
   Naval Postgraduate School
   Monterey, California

5. Douglas C. Loup
   Naval Surface Warfare Center, Carderock Division
   West Bethesda, Maryland

6. Erik A. Rasmussen
   Naval Surface Warfare Center, Carderock Division
   West Bethesda, Maryland

7. Scott W. Bartlett
   Naval Surface Warfare Center, Carderock Division
   West Bethesda, Maryland

8. Engineering and Technology Circular Office, Code 34
   Naval Postgraduate School
   Monterey, California

9. Michael A. Violette
   Naval Postgraduate School
   Monterey, California